JOURNAL OF NEUROTRAUMA 35:2883–2903 (December 15, 2018)

DOI: 10.1089/neu.2017.5439

Transplantation of Neural Progenitors and V2a Interneurons after Spinal Cord Injury

Lyandysha V. Zholudeva,[1,2] Nisha Iyer,[3] Liang Qiang,[1,2] Victoria M. Spruance,[1,2] Margo L. Randelman,[1,2] Nicholas W. White,[4] Tatiana Bezdudnaya,[1,2] Itzhak Fischer,[1,2] Shelly E. Sakiyama-Elbert,[4] and Michael A. Lane[1,2]

Abstract

There is growing interest in the use of neural precursor cells to treat spinal cord injury (SCI). Despite extensive pre-clinical research, it remains unclear as to which donor neuron phenotypes are available for transplantation, whether the same populations exist across different sources of donor tissue (e.g., developing tissue vs. cultured cells), and whether donor cells retain their phenotype once transplanted into the hostile internal milieu of the injured adult spinal cord. In addition, while functional improvements have been reported after neural precursor transplantation post-SCI, the extent of recovery is limited and variable. The present work begins to address these issues by harnessing ventrally derived excitatory pre-motor V2a spinal interneurons (SpINs) to repair the phrenic motor circuit after cervical SCI. Recent studies have demonstrated that Chx10-positive V2a SpINs contribute to anatomical plasticity within the phrenic circuitry after cervical SCI, thus identifying them as a therapeutic candidate. Building upon this discovery, the present work tests the hypothesis that transplantation of neural progenitor cells (NPCs) enriched with V2a INs can contribute to neural networks that promote repair and enhance respiratory plasticity after cervical SCI. Cultured NPCs (neuronal and glial restricted progenitor cells) isolated from E13.5 Green fluorescent protein rats were aggregated with TdTomato-mouse embryonic stem cell–derived V2a INs *in vitro*, then transplanted into the injured cervical (C3-4) spinal cord. Donor cells survive, differentiate and integrate with the host spinal cord. Functional diaphragm electromyography indicated recovery 1 month following treatment in transplant recipients. Animals that received donor cells enriched with V2a INs showed significantly greater functional improvement than animals that received NPCs alone. The results from this study offer insight into the neuronal phenotypes that might be effective for (re)establishing neuronal circuits in the injured adult central nervous system.

Keywords: interneuron; neural progenitor; spinal cord injury; transplantation; V2a interneurons

Introduction

There is a growing appreciation for the endogenous neuroplastic potential of the injured spinal cord. For example, within the respiratory system, spontaneous recovery of phrenic function has been observed weeks[1–5] to months[6,7] after a high cervical spinal cord injury (SCI). One key component to functional motor and sensory neuroplasticity post-SCI appears to be the recruitment of spinal interneurons (SpINs) into novel circuits.[8–14] While the role of SpINs in respiratory plasticity remains unknown, the V2a class of glutamatergic neurons in the brainstem and the spinal cord has both direct and indirect influences on respiratory and non-respiratory motor neurons.[15–22] Thus, these SpINs serve as an attractive candidate for the formation of novel circuits after SCI, especially since glutamate has been demonstrated to play an important role in recovery after high cervical SCI.[23–25] Excitatory SpINs also have been shown to become functionally recruited using intermittent hypoxia (a means of entraining respiratory plasticity)[26] and more recently, it has been demonstrated that they can be harnessed to drive respiratory output in the absence of all medullar input.[27] Further, ablation of V2a INs results in abnormal respiratory patterns.[19] V2a INs also play a crucial role in the neuroplastic activation of accessory respiratory muscles during progression of amyotrophic lateral sclerosis,[22] and have been demonstrated to become anatomically recruited into the phrenic motor circuit after high cervical SCI.[13]

Despite the neuroplastic potential for recovery after hemisection[1,13,28] or contusion injuries,[1,12,28–30] substantial respiratory deficits persist. In addition to compromised bulbospinal input to phrenic motor neurons,[12] contusive injuries also result in direct loss of SpINs

[1]Department of Neurobiology and Anatomy, [2]Spinal Cord Research Center, College of Medicine, Drexel University, Philadelphia, Pennsylvania.
[3]Wisconsin Institute for Discovery, University of Wisconsin, Madison, Wisconsin.
[4]Department of Biomedical Engineering, University of Texas, Austin, Texas.

post-injury[31–33] that may contribute to the respiratory deficits seen or limit neuroplastic potential. The present work explores whether transplantation of SpIN-rich neural progenitor cells (NPCs) can provide the injured cervical spinal cord with neuronal components to facilitate anatomical repair and promote plasticity.

Transplantation of freshly dissected,[34–41] trypsinized,[42,43] or cultured[42,44,45] neural precursor cells derived from the embryonic (E13-14) rat spinal cord has been identified as a promising therapeutic strategy for replacing lost or damaged spinal neurons and glia after SCI. Numerous sources for NPCs have been identified and tested for SCI repair,[46,47] but the cells used in this study were harvested and cultured from E13-14 rat spinal cord.[48] Prior to cell culture, the E14 spinal cord contains approximately 80–90% of neuronal and glial restricted progenitor cells (or collectively,NPCs) and 10% neuroepithelial cells, post-mitotic neuronal cells, and non-neural cells.[49,50] Adherent culture refines this diverse population to produce neuronal and glial restricted progenitors. Previous work has shown that transplanted freshly dissected tissues are innervated by the host, become synaptically integrated with the injured phrenic circuitry, and can modulate phrenic motor output,[38–40] but whether cultured NPCs can recapitulate these outcomes within the phrenic circuit has not been explored.

The present study assessed whether transplanting NPCs alone or enriched with glutamatergic V2a INs into the cystic cavity that forms after a contusive SCI in the adult rat can contribute to functional circuit recovery. Here, we demonstrate the survival, proliferation, and integration of these transplanted cells, and their contribution to phrenic (diaphragm) recovery 1 month after transplantation. Importantly, we found transplanted post-mitotic interneurons survive alongside transplanted NPCs and extend neurites (putative axons) up to several millimeters outside lesioned tissue. Migration of donor glia (from green fluorescent protein [GFP]-positive donor NPCs) also was observed both rostrally and caudally several millimeters outside of lesioned tissue. A population of transplanted V2a INs matured and expressed NeuN with no detection of glial fibrillary acidic protein (GFAP) expression, while NPCs expressed both neuronal (NeuN) and glial (GFAP) markers. Further, terminal diaphragm electromyography (dEMG) recordings from these studies demonstrate greater baseline output and improved response to challenge in recipients of V2a INs, compared with vehicle and NPC-only–treated animals. With growing evidence that SpINs play a critical role in plasticity[9,12–14,26,51–53] and functional circuit remodeling following SCI,[8,9,54–56] the results from this work offer important insights into how specific neuronal subtypes can be harnessed for treatment of the injured adult spinal cord.

Methods

Adult female, Sprague-Dawley rats ($n = 48$; 250–280 g; Envigo®) were housed at the Drexel University College of Medicine animal care facility. Experimental procedures were conducted with approval from the Institutional Animal Care and Use Committee and following the National Research Council Guidelines for the Care and Use of Laboratory Animals. All animals received a lateralized moderate contusive spinal cord injury (SCI) located at cervical levels 3–4, which results in the loss of phrenic motoneurons and spinal interneurons (SpINs) as well as persistent respiratory deficits as measured by response to respiratory challenges (hypoxia, hypercapnia). Animals were blindly separated into one of three groups (vehicle, NPCs, or NPC/V2a INs) and decoded at the end of experiments and analysis. V2a INs were engineered from mouse embryonic stem cells,[57] whereas NPCs were derived from the developing rat spinal cord (E13.5 rat).[48] NPCs were injected as either single cells or were aggregated for 2 days prior to injection. V2a INs were combined with NPCs *in vitro* for 2 days to form NPC-V2a cellular aggregates, which were then injected into the contused spinal cord.

Preparation of NPCs

Spinal cord tissue was dissected from E13.5 Fischer 344 GFP or alkaline phosphatase (AP) transgenic rat embryos, obtained from time-mated dams. NPCs were derived from the mechanically and enzymatically (Trypsin; Life Technologies #25200-056) dissociated spinal cord tissues and cultured as previously described,[48] and stored in liquid nitrogen until needed. Cells were thawed 1 day prior to aggregation by seeding 3×10^6 NPCs onto poly-L-lysine (Sigma-Aldrich, #P8920) and laminin (ThermoFisher, #23017015) coated T75 flasks and cultured in NPC Medium comprised of: DMEM/F12 containing 25 mg/mL bovine serum albumin, B-27 supplement (Life Technologies, #17504-044), N2 supplement (Life Technologies, #17502-048), 10 ng/mL basic fibroblast growth factor (bFGF; Peprotech, #450-10, Rocky Hill, NJ), and 20 ng/mL neurotrophin-3 (NT-3; Peprotech, #450-03; Fig. 1A).

Neural inductions from selectable embryonic stem cell lines

A selectable Chx10-Puro mouse embryonic stem cell (ESC) line constitutively expressing TdTomato was cultured and differentiated as previously described[57] to produce V2a INs. ESCs were cultured on gelatin-coated T75 flasks in complete media containing 1000 U/mL leukemia inhibitory factor (Millipore, #ESG1106) and 100 μM β-mercaptoethanol (Life Technologies, #21985-023). The cell line was differentiated using a $2^-/4^+$ induction protocol (Fig. 1B). On Day 0, 1×10^6 ESCs were seeded into 10 mL of DFK5 media on an agar-coated 100 mm petri dish for 2 days to form embryoid bodies (EBs). On Day 2, the media was replenished with DFK5 containing 10 nM retinoic acid (Sigma, #R2625) and 1 μM purmorphamine (EMD Millipore, #540223); on Day 4, the media were replaced with DFK5 containing 10 nM RA, 1 μM purmorphamine and 5 μM (N-N-(3,5-difluorophenacetyl-L-alanyl)-(S)-phenylglycine-t-butyl-ester) (DAPT; Sigma, #D5942). EBs were dissociated and re-suspended in a selection media of DFK5NB containing B-27 supplement, glutaMAX (Life Technologies, #35050-061), 5 ng/mL glial-derived neurotrophic factor (Peprotech, #450-10), 5 ng/mL brain derived neurotrophic factor (BDNF; Peprotech, #450-02), 5 ng/mL NT-3, and 4 μg/mL puromycin in water (Sigma, #P8833). Differentiated Chx10-Puro cells were plated on laminin coated T75 flasks at a density of 5×10^5 in the selection media for 24 h (Fig. 1B).

Preparation of aggregates for transplantation

NPCs and V2a INs were lifted from laminin-coated flasks using Accutase (Sigma, #A6964) for 30 min at room temperature; 5×10^5 cells were seeded into each well of a 400-μm AggreWell plate (StemCell Technologies, #27845) for 2 days in NPC Media to form aggregates for transplantation (Fig. 1C-E). Mixed groups were seeded at a 1:1 ratio, to make a total of 5×10^5 cells per well, and half the media were replaced daily. Aggregates were resuspended by trituration and allowed to settle in microcentrifuge tubes (Fig. 1F). The media were aspirated, and the cells washed once with Hank's Balanced Salt Solution (HBSS; ThermoFisher, #14025076) prior to transplantation or *in vitro* characterization.

Characterization of NPCs in vitro (2D culture)

At the time of NPC aggregation with V2a INs, a subset of NPCs (50,000 cells/cover-slip) were plated onto poly-L-lysine and laminin coated 25 mm^2 glass cover-slips and allowed to attach for 10 h prior to live-cell immunocytochemistry or fixation with paraformaldehyde (4%) for 10 min and staining. Live cell immunocytochemistry was used to confirm the previously published

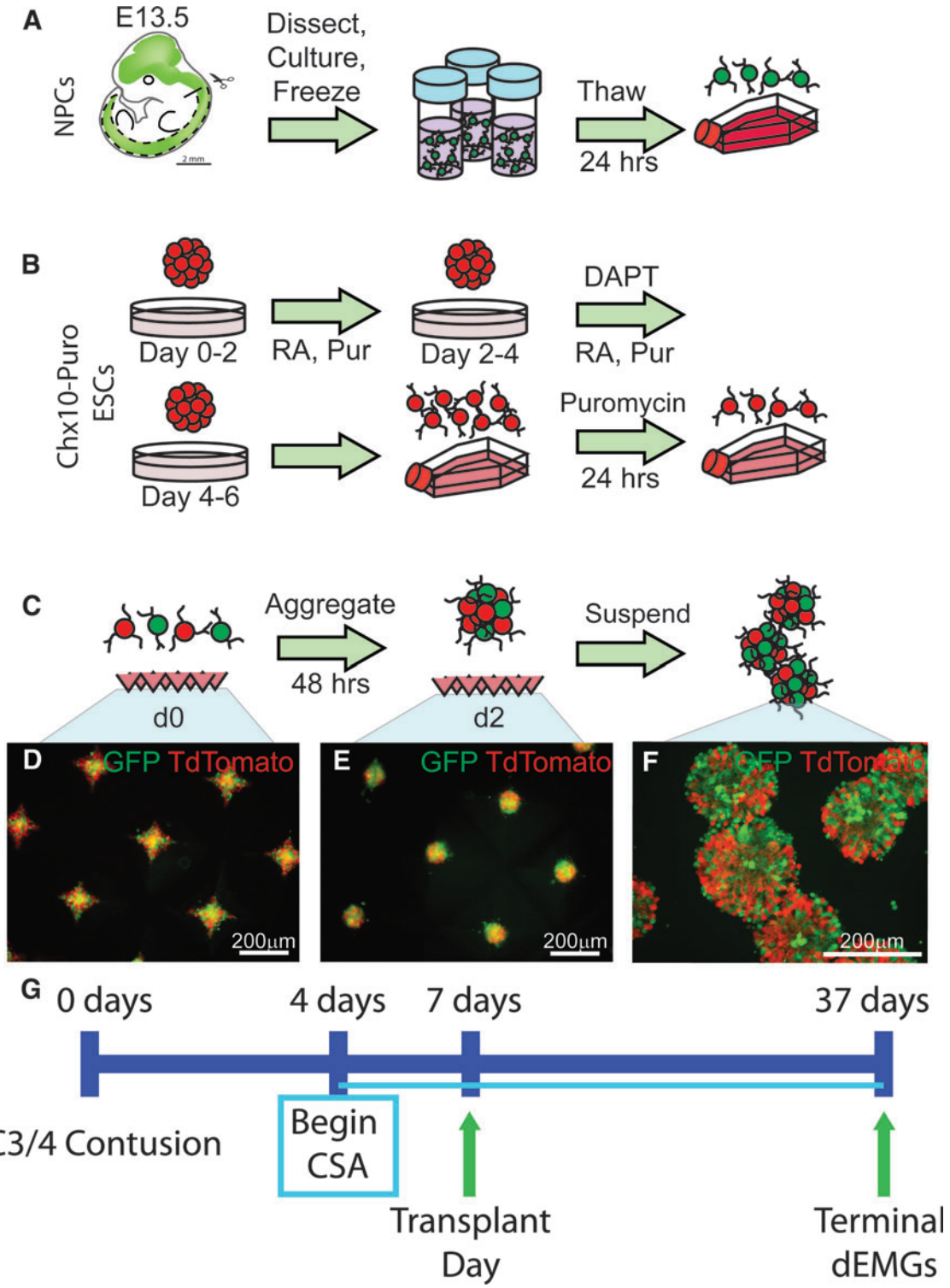

FIG. 1. Generation and aggregation of neural progenitor cells (NPCs) and V2a interneurons (INs). **(A)** NPCs isolated from E13.5 rat spinal cords were stored frozen and thawed 1 day prior to aggregation. **(B)** Chx10-Puro embryonic stem cells (ESCs) expressing TdTomato were induced using a $2^{-}/4^{+}$ protocol followed by 24 h of puromycin selection for V2a INs. **(C)** Schematic showing aggregation protocol. Populations of NPCs were mixed at a 1:1 ratio with TdTomato-V2a cells and seeded into an AggreWell plate. After 2 days of culture, spherical aggregates form in the dish (green fluorescent protein/TdTomato, NPC/V2a INs, respectively shown in **D-F**), which are then resuspended in fresh media and washed in Hank's Balanced Salt Solution prior to transplantation (F). Scale bars are as indicated. **(G)** Experimental timeline of the study.

characteristics of NPCs used for transplantation in this study. As previously described,[48] neuronal and glial restricted progenitor cells were labeled with surface markers E-NCAM and A2B5, respectively (Fig. 2A-E). Briefly, after aspirating the culture media, cells were washed with 37°C HBSS prior to application of primary antibody (Table 1) diluted in 37°C NPC Medium (see above). Cells were incubated with primary antibody at 37°C and 5% CO_2 for 30 min before the media were aspirated and the cells were washed with 37°C HBSS three times. Secondary antibodies (Table 1) diluted in NPC Medium were applied to cells and cells were incubated at 37°C and 5% CO_2 for 30 min prior to three washes with 37°C HBSS. Cells were then fixed with 4% paraformaldehyde for 10 min before three washes with phosphate-buffered saline (PBS; ThermoFisher, #10010023) and a 10-min incubation with PBS containing 4′,6-diamidino-2-phenylindole, dihydrochloride (1:1000; DAPI; ThermoFisher, #D1306). Cover-slips were secured onto slides with fluorescence mounting medium (Dako Agilent, #S302380-2) and imaged using a Zeiss AxioImager microscope with a Zeiss Axiocam MRm camera, attached to a Dell PC.

All other immunocytochemistry was performed on fixed cells (4% paraformaldehyde for 10 min). Fixed cells were washed with PBS prior to blocking with normal donkey serum (GeneTex, #GTX73205) and 0.01% Triton (EMD Millipore, #9036-19-5) for 1 h. Cells were stained with primary antibody overnight (Table 1), washed three times with PBS, and stained with appropriate secondary antibody (able 1). Cells were then washed three times for 5 min with PBS prior to a 10-min incubation with PBS containing DAPI as above. Cover-slips were secured onto slides with fluorescence mounting medium (Dako Agilent, #S302380-2) and imaged using a Zeiss AxioImager microscope with a Zeiss Axiocam MRm camera, attached to a Dell PC. Counting of Chx10-positive cells (Fig. 2F) was performed in ImageJ software (National Institutes of Health [NIH], Bethesda, MD) with approximately 200 cells counted (as determined by DAPI staining) per replicate ($n=6$).

Quantitative real-time polymerase chain reaction (qRT-PCR)

Three different groups of cultured NPCs were analyzed and compared with fetal spinal cord tissue (FSC): NPCs that were thawed and plated onto poly-L-lysine and laminin coated T75 flask for 12 h (equivalent to non-aggregated transplanted NPCs) or 2 days (2DIV, 2D), as well as NPC aggregates (2DIV, 3D culture; equivalent to transplanted NPC aggregates). All samples were lysed and RNA was extracted using the Qiagen RNeasy kit (Qiagen, #74104). The complementary DNA (cDNA) was synthesized using a high capacity RNA to cDNA kit (ThermoFisher, #4368814) and combined with TaqMan Gene Expression Assays and TaqMan Fast Advanced Master Mix (Applied Biosystems, #4444963). qRT-PCR was performed using a QuantStudio 3 (Applied Biosystems, CA) thermocycler with the following protocol: 95°C for 20 sec; 40 cycles of 95°C for 1 sec, and 60°C for 20 sec. Expression of transcription factor messenger RNA (mRNA) of Evx1, En1, Chx10, Lhx3, and Hb9 was assessed in each NPC sample described above and compared with level of expression in embryonic (E13.5) spinal cord tissue (FSC) and graphically represented as a percent relative to expression in FSC, with FSC levels set as 100%. The list of primers used is included in Table 2. There were $n=3$ technical replicates completed per run and $n=3$ biological replicates for each sample.

Characterization of V2a INs within NPC-V2a aggregates in vitro (3D culture)

Average diameter and distribution of NPCs (GFP labeled) and V2a INs (TdTomato labeled) were determined using phase and fluorescent images, respectively, and quantified using ImageJ. Fluorescent images of aggregates were obtained by placing the aggregates between glass cover-slips and imaging using a MICROfire camera attached to an Olympus IX70 inverted microscope (Fig. 1F). To determine cell viability, aggregates were prepared using an ESC line that does not contain a fluorescent reporter, whereas GFP expression in rat NPCs was sufficiently low enough to achieve threshold for analysis. Aggregates were incubated in Accutase for 3 h at room temperature with agitation, then triturated to dissociate. Single cells were then incubated for 30 min in PBS containing calcein-AM and ethidium homodimer-1 (Life Technologies, #C481) to stain alive and dead/dying cells prior to imaging. Counting was performed in ImageJ, with approximately 300 cells counted per replicate ($n=3$). Fluorescent aggregates were similarly dissociated and quantified to determine the population distribution within mixed groups.

Surgical methods

All animals were anesthetized by injection of xylazine (10 mg/kg, s.q.) and ketamine (120 mg/kg, i.p.) for spinal cord injury, transplantation and electrophysiology procedures. Spinal cord injured and vehicle treated animals also underwent neuroanatomical tracing under isoflurane anesthesia (4% in 100% O_2 to induce, 2% in 100% O_2 to maintain). Upon completion of each procedure, xylazine-induced anesthesia was reversed via injection of yohimbine (1.2 mg/kg s.q.). Post-operative medicine included lactated Ringer's (5 mL, s.q.) to prevent dehydration and buprenorphine (0.025 mg/kg s.q.) was used as an analgesic.

SCI

For SCI, animals were prepared for surgery as previously described.[12] Briefly, a skin incision was made with a No. 15 scalpel blade from the base of the skull to the fifth cervical segment (C5), surrounding musculature was carefully cut and pushed apart and a laminectomy was made at the third cervical segment (C3) and rostral part of C4. Animals were secured with vertebral clamps at the C2 process and C4 process, slightly elevating the animal from the surgical frame. All animals received a lateralized contusion injury just caudal to C3 dorsal root on the left side of the spinal cord using a 2 mm tip attached to the Infinite Horizon Pneumatic Impactor (Precision Systems, Lexington, KY), with the height of the tip preset to 5 mm and impact force preset to 200 kilodynes and zero dwell time. All animals that experienced respiratory arrest were intubated using a 16-gauge catheter (Braun Medical Inc., #4251695-02) attached to a fiber optic light and mechanically ventilated (Small Animal Ventilator; Harvard Apparatus) for 1 h. The underlying muscle was sutured in layers and the skin was closed with wound clips just prior to administration of post-operative medicine.

Transplantation

All animals were immunosuppressed with cyclosporin A (10 mg/kg daily s.q.), starting three days prior to transplantation and throughout the duration of the study (Fig. 1G). Animals were blindly separated into one of three groups (vehicle, NPCs, or NPC/V2a INs) and decoded after all functional data analysis. Animals were anesthetized as described above and the skin and underlying musculature were re-exposed 1 week post-injury. Using a 33-gauge needle tip, a small hole was made in the dura overlying the epicenter of the injury (visualized by the bruise in the spinal tissue). Non-aggregated (single-cell suspension) NPCs (5×10^5 cells per animal; $n=8$), NPC aggregates (5×10^5 cells per animal; $n=6$) or NPC/V2a IN aggregates (5×10^5 cells per animal prepared in a 1:1 ratio as described above; $n=8$) were injected into the contusion cavity via a gas tight 25 uL Hamilton syringe with a custom 30-gauge needle attached to a micromanipulator (Model Kite-L; World Precision Instruments). Age-matched controls ($n=8$) received all the described surgical procedures, but instead of a cellular injection, received an equal volume (6 uL) of HBSS into the lesion cavity. The underlying muscle

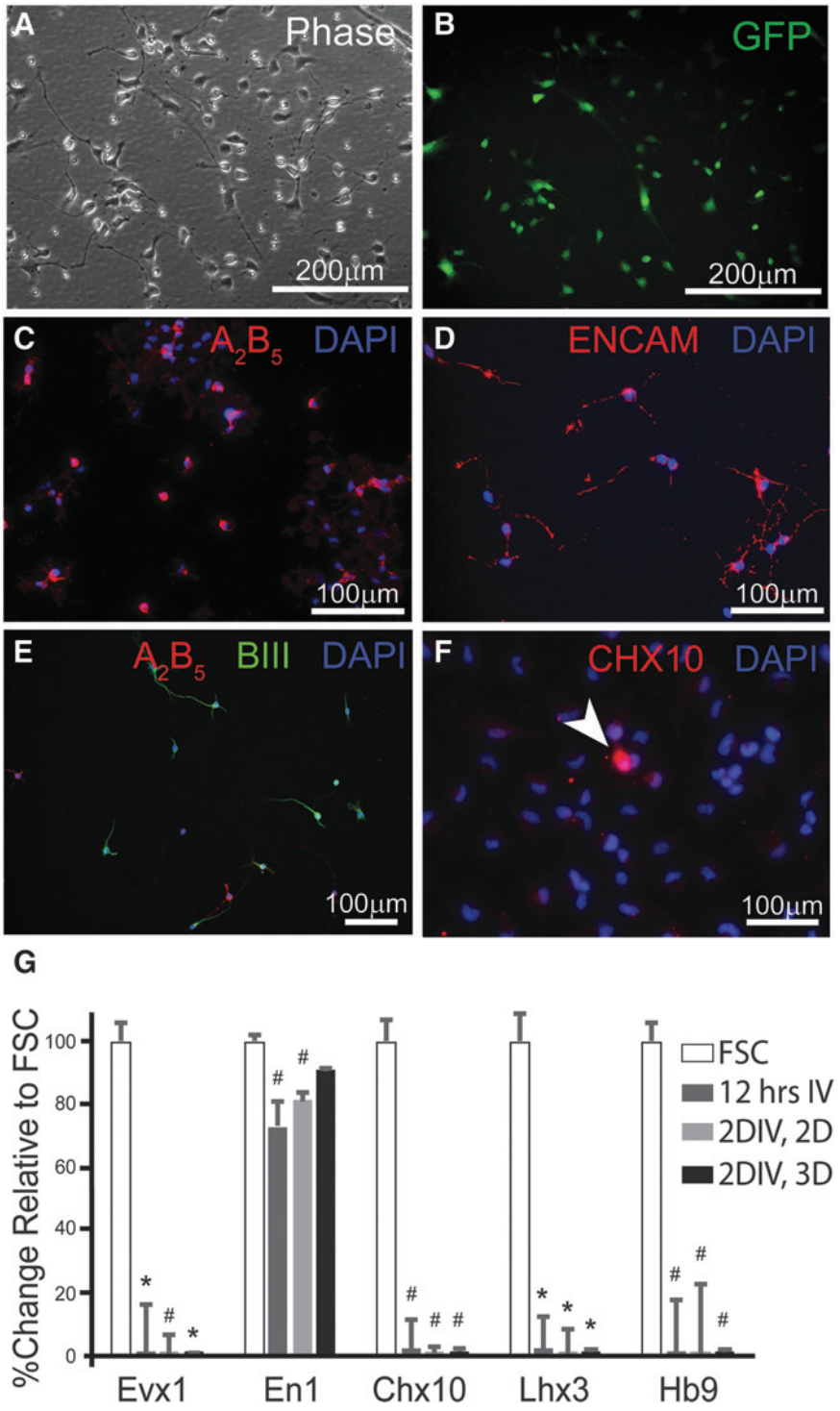

FIG. 2. *In vitro* characterization of neural progenitor cells (NPCs). Phase **(A)** and fluorescence **(B)** images of NPCs show morphology typical of progenitor neurons and glia after isolation, culturing, freezing, and thawing procedures. Live-cell immunocytochemistry against A_2B_5 **(C)** and ENCAM **(D)** demonstrates the presence of both glial and neuronal progenitor cells, respectively, with some expression of βIII Tubulin **(E).** Immunocytochemistry against the transcriptional factor Chx10, a marker for V2a interneurons (INs), reveals a small population of NPCs that express the protein **(F).** Messenger RNA (mRNA) was isolated from NPCs thawed and cultured for 12 h on adherent, 2-dimensional flask (2D), for 2 days *in vitro* (2DIV, 2D) and from NPC aggregates, which are cultured in suspension or ''3D'' (2DIV, 3D). Quantitative real-time polymerase chain reaction analysis of these mRNA samples reveals decreased transcription of ventral IN markers (Evx1, Chx10, Lhx3, Hb9), compared with mRNA isolated from fetal spinal cord (FSC) tissue (expressed as 100%). NPCs cultured for 12 h and 2 days, but not for 2 days as aggregates have lower expression of En1 compared with mRNA in FSC samples. Scale bars are as indicated. Two-tailed Student's *t*-test: $*p < 0.0001$ and $\#p < 0.05$ compared with FSC group.

Table 1. List of Primary and Secondary Antibodies

Host	*Antigen*	*Concentration*	*Vendor*	*Catalogue number*
Primary antibodies				
Chicken	GFP	1:700 IHC	Abcam	Ab13970
Mouse	NeuN	1:200 IHC	Millipore	MAB377
Mouse	Nestin	1:1000 IHC	BD Pharmigen	556309
Mouse	GFAP	1:400 IHC	Millipore	MAB360
Mouse	Synaptophysin	1:1000 IHC	Synaptic Systems	101 011
Mouse	GAD67	1:500 IHC	Millipore	MAB5406
Mouse	vGlut1	1:1000 IHC	Millipore	MAB5502
Mouse	ENCAM	1:2 ICC	DSHB	
Mouse	A_2B_5	1:2 ICC	DSHB	
Rabbit	PRV	1:10,000 IHC	Courtesy of Lynn Enquist, Princeton University	
Rabbit	NeuN	1:500 IHC	Abcam	Ab177487
Rabbit	Ki67	1:200 IHC	ThermoFischer	PA5-16785
Rabbit	ßIII Tubulin	1:1000 ICC	Abcam	Ab18207
Sheep	CHX10	1:200 ICC	Millipore	AB9016
Secondary antibodies				
Anti-chicken	Alexa Fluor 488	1:200 IHC	ThermoFischer	A-11039
Anti-mouse	Alexa Fluor 647	1:200 IHC	Molecular Probes	A31571
Anti-mouse	DyLight 405	1:200 IHC	Jackson ImmunoResearch	715-475-150
Anti-rabbit	DyLight 405	1:200 IHC	Jackson ImmunoResearch	711-475-152
Anti-mouse	DyLight 594	1:400 ICC; 1:200 IHC	Jackson ImmunoResearch	715-515-150
Anti-rabbit	Alexa Fluor 488	1:400 ICC	Invitrogen/ ThermoFischer	A21206
Anti-sheep	Alexa Fluor 594	1:400 ICC	Jackson ImmunoResearch	713-585-003

GFP, green fluorescent protein; IHC, immunohistochemistry; GFAP, glial fibrillary acidic protein; ICC, immunocytochemistry.

was sutured in layers and the skin was closed with wound clips prior to administration of post-operative medicine. Animals recovered for 1 month prior to terminal electrophysiology recordings. A separate group of injured animals received single-cell suspension AP NPCs (5×10^5 cells per animal; $n=5$) and sacrificed at 3 days ($n=2$), 1 week ($n=2$), and 2 weeks ($n=1$) post-transplant.

Neuroanatomical tracing

A transynaptic retrograde tracing technique (pseudorabies virus [PRV]) was used to label the phrenic motor circuit and confirm the location and severity of the injury, 1 month after injury as previously described.[58] Briefly, after reaching a surgical plane of isoflurane-induced anesthesia, a laparotomy was performed to expose the diaphragm and a Bartha strain of PRV (50 uL total volume) was topically applied onto the hemidiaphragm ipsilateral to injury. The PRV recombinant used in this study was PRV 614 (8.0–9.9×10^8 pfu/mL) expressing red fluorescent protein. PRV614 was supplied to us by Dr. David Bloom, University of Florida.

Table 2. Primers Used for qRT-PCR Characterization of Cultured NPCs and FSC Tissue

Taqman probe	*Reporter*	*Quench*	*Assay number*	*Catalogue #*
Evx1	FAM	MGB	Mm00433154_m1	4331182
En1	FAM	MGB	Mm00438709_m1	4351370
Chx10	FAM	MGB	Mm00432549_m1	4331182
Hb9	FAM	MGB	Mm01222622_m1	4331182
Lhx3	FAM	MGB	Mm01330619_g1	4351372
Actb	VIC_PL	MGB	Mm02619580_g1	4448485

qRT-PCR, quantitative real-time polymerase chain reaction; NPCs, neural progenitor cells; FSC, fetal spinal cord.

Diaphragm electromyography

Terminal, bilateral dEMG recordings were performed on every animal as described elsewhere[12] just prior to being euthanized and perfusion-fixed for histological analyses. Briefly, animals were anesthetized with a mixture of xylazine and ketamine and a laparotomy was performed to expose the abdominal surface of the diaphragm. Bipolar hook electrodes (PFA coated tungsten wire with exposed tips; A-M Systems, #796500) were then placed into the medial costal region of the left and right hemidiaphragm as previously described.[12] Pulse oximetry was used to assess change in blood oxygen saturation using a collar cuff (Part #: 015023) and MouseOx (Starr Life Sciences Corp.). Diaphragm activity was recorded during spontaneous breathing and baseline was counted as a minimum of 10 min of stable activity with an oxygen saturation of 90–98%. Once baseline was acquired, a nose cone was placed over the animals' nose, which allowed the administration of hypercapnic (7% CO_2, balanced in N_2; flow rate 2 L/min) or hypoxic gas (10% O_2, balanced in N_2; flow rate 2 L/min), as means of a 5-min respiratory challenge. The purpose of the 5-min respiratory challenges is to test the ability of the animals (injured and injured with transplant) to increase muscle output and subsequent ventilation upon increased demand. This method of increasing the respiratory drive can reveal functional deficits that are not evident during a period of quiet, eupneic breathing (e.g. baseline).[59] The dEMG signals were amplified (1000×) and band pass filtered (0.3–5 KHz) using differential A/C amplifier (Model 1700; A-M Systems) and digitized (Power 1401; Cambridge Electronic Design).

Immunohistochemistry

At the end of terminal recordings, all animals were intracardially perfused with physiological saline (0.9% NaCl in water) and paraformaldehyde (4% w/v in 0.1 M PBS; pH 7.4). The spinal cords were then removed and stored in 4% paraformaldehyde overnight. Spinal cord tissue spanning caudal-most part of brainstem to beginning of thoracic spinal cord (T1-2) was cryoprotected (15%,

then 30% sucrose, overnight), and sectioned (on-slide 20 μm or 30 μm, transverse or longitudinal, respectively) using a cryostat.

Sections were rehydrated for 15 min in PBS, blocked against endogenous peroxidase activity (30% methanol, 0.6% hydrogen peroxide in 0.1 M PBS, incubated for 1 h), and blocked against nonspecific protein labeling (10% serum in 0.1 M PBS with 0.02% Triton-X, incubated for 1 h), prior to application of primary antibodies in blocking solution. Primary antibodies (Table 1) were left on the tissue overnight at room temperature. Antibodies to PRV were supplied by Dr. Lyn Enquist (Princeton University, NJ). The following day, tissue was washed in PBS (0.1 M, 3×5 min) and incubated in blocking solution with secondary antibodies (Table 1). Immunolabeled sections were then washed in PBS (0.1 M, 3×5 min), allowed to dry, and cover-slipped with fluorescence mounting medium (Dako). Sections were examined using a Zeiss AxioImager microscope with Apotome 2 attached to a Dell PC. Photographs were taken with a digital camera (Zeiss Axiocam MRm) or with a Leica TCS SP8 with DMi8 inverted optical stand (63β objective lens).

Anatomical and functional data analysis

Diaphragm electromyography traces were integrated (DC bias removed at 0.1 sec), rectified and smoothed (0.03 sec) using Spike 2 software (version 8; Cambridge Electronic Design, UK). Baseline diaphragm output was determined during eupneic breathing by averaging integrated signal over a 40-sec interval immediately before a respiratory challenge. Diaphragm output during a respiratory challenge was determined by averaging integrated signal over a 40-sec interval at the end of each 5-min challenges. The average maximum voltage and percent change of each challenge from baseline breathing was determined from the averaged, integrated signal for each respiratory state using OriginPro9 software (Northampton, MA). Results are reported as average $\pm$ standard error, or as percent change relative to baseline (eupnea) where indicated. Statistical analyses were performed using SPSS (IBM SPSS Statistics 23). Comparison between vehicle and transplant recipients was made using analysis of variance (ANOVA) and Student *t*-test (IBM SPSS Statistics 23). All analyses of electrophysiological data were blinded.

Transplant survival was determined as the volume of GFP-positive labeling within the volume of lesioned tissue between serial sections 90 μm apart. To estimate the volume of the transplant and lesioned tissue between two serial sections, the area of the transplant or lesion was multiplied by the distance between each section. Half of the difference between the two volumes was then added to the volume measured for the section with the smaller measured area, giving an estimate of the volume between two sections. The area of the transplant was defined as area occupied by green labeled cells with a threshold set based on presence of positive GFP signal while excluding background noise using ImageJ. Lesioned area for each section was manually determined in ImageJ by the presence of clearly identifiable macrophages, tissue debris, presence of empty cavity space, or a clearly defined transplant–host integration zone. The integration zone is defined as the intermingling of host and donor cells. Results are reported as average percent of transplant volume per volume of lesioned tissue $\pm$ standard error.

The number of TdTomato positive V2a INs (TdTomato only), NeuN positive V2a INs (NeuN/TdTomato double labeled), and NeuN positive NPC INs (GFP/NeuN double labeled) were manually counted in 12 sections, 90 μm apart to avoid double counting cells, per animal ($n=5$). To estimate the total number of cells within a transplant, the number of cells counted in a section was multiplied by the thickness between sections used for cell counts. Feret diameter maximum (the longest diameter measured for each circled cell) for the three types of interneurons (V2a INs, V2a INs that are positive for NeuN, and NPCs positive for NeuN) and migrating glial cells were determined with Zen Blue software. Results are reported as average Feret diameter (μm) $\pm$ standard error. Statistical analyses were performed using SPSS (IBM SPSS Statistics 23). Comparison between vehicle and transplant recipients was made using ANOVA and Student's *t*-test.

Results

In vitro characterization of donor cell populations

NPCs were dissected from E13.5 spinal cord of transgenic GFP rats, cultured, and frozen as previously described (Fig. 1A).[48] V2a interneurons (INs) were derived from Chx10-Puromycin–resistant embryonic stem cells (ESCs; Fig. 1B), and aggregated for 2 days with NPCs (Fig. 1C-E). The aggregates were then suspended in HBSS (Fig. 1F) prior to transplantation into cervically (C3/4) contused animals, 1 week after injury (Fig. 1G). NPCs were comprised of E-NCAM positive neuronal restricted progenitors (NCAM1 specific to rat embryonic spinal cord membranes), and A_2B_5 positive glial restricted progenitor cells, with a portion of cells that expressed ßIII tubulin (Fig. 2A-E), as previously demonstrated.[48,60] Quantification of the number of Chx10-positive cells (marker for V2a interneurons, INs) within cultured NPCs (12 h) revealed 7.75 $\pm$ 0.3% of all cells present positive for Chx10 antibody (Fig. 2F).To further characterize ventrally-derived IN subtypes present in cultured NPCs, qRT-PCR analysis was performed for Evx1 (V0 INs), En1 (V1 INs), Chx10 and Lhx3 (V2a INs), and Hb9 (motoneurons and Vx INs). Analysis revealed significantly lower mRNA levels of Evx1, Chx10, Lhx3, and Hb9 compared with freshly dissected E13.5 spinal cord tissue (FSC) in all cultured NPC conditions (Fig. 2G), including NPCs cultured for 12 h, 2 days (2DIV, 2D), and 2 days as aggregates (2DIV, 3D). mRNA level of En1 was significantly decreased in NPCs cultured for 12 h and 2DIV, 2D but not as aggregates (Fig. 2G).

V2a INs labeled with TdTomato were derived from embryonic stem cells (ESCs) as previously described[57] by a process of differentiation and selection (Fig. 3A, 3B). As characterized and reported previously,[57] the puromycin selection results in generation of highly enriched V2a INs, of which 80% are Chx10+ with 94% Lhx3+ (Fig. 3C, modified from Iyer and colleagues).[57] When cocultured with glia and motor neurons these V2a INs mature into glutamatergic neurons, confirmed with molecular markers and electrophysiology *in vitro*.[57] As such, selected V2a INs were combined with NPCs via aggregation to provide physical and trophic support to the post-mitotic V2a INs, then cultured for 2 days in AggreWell plates to form stable aggregates that demonstrate interpenetrating networks of neurites (Fig. 1D-F). Although mixed groups were seeded at a 1:1 ratio, proliferation in NPC populations during the aggregation process resulted in a V2a population of 36.55 $\pm$ 1.63% in the aggregates, which still represented about a 5-fold enrichment over the NPC population alone. The size difference between aggregates can be ascribed to this proliferation; groups containing NPCs averaged 125.55 $\pm$ 16.05 μm in diameter, NPC/V2a INs averaged at 124.35 $\pm$ 20.09 μm in diameter and V2a IN aggregates were slightly smaller (104.9 $\pm$ 14.63 μm; Table 3). To determine cell viability, aggregates were enzymatically dissociated by incubation in Accutase. Despite shear caused by trituration, all groups contained greater than 90% live cells (Table 3).

Respiratory deficits following cervical spinal cord injury

The spinal cord injury (SCI) used in this study is a high cervical (C3/4), moderate-severe injury that resulted in both white and gray matter damage around the phrenic motor pool (C3-6, Fig. 4A). A total of 48 animals received a lateralized contusion injury with the

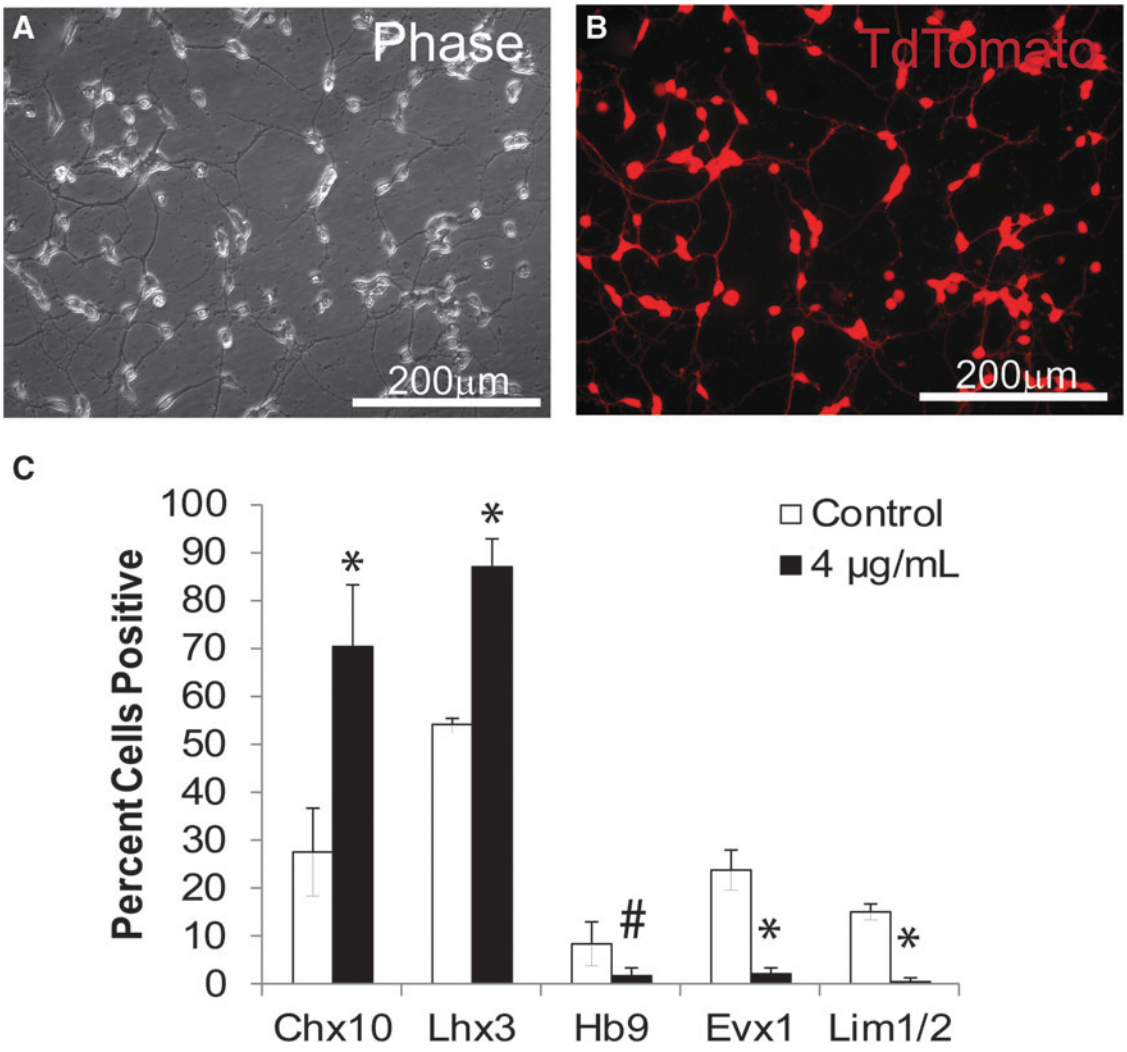

FIG. 3. *In vitro* characterization of V2a interneurons (INs). V2a INs generated from Chx10-Puro embryonic stem cells (ESCs) have morphological features of post-mitotic neurons as described previously,[56] and shown in phase **(A)** and fluorescence **(B)** images. **(C)** Flow cytometry analysis of ventral Chx10-Puro ESCs derived and selected IN subpopulations in control and puromycin-selected cultures. $*p < 0.0001$ compared with control group $\#p < 0.05$ compared with control group.

TABLE 3. QUANTIFICATION OF CELL VIABILITY, POPULATION DISTRIBUTIONS, AND AGGREGATE SIZES

	% Cell viability	*% V2a*	*Diameter (μm)*	*# Aggregates*
NPC Aggs	94.61 ± 0.87	0	125.55 ± 16.05	512
V2a Aggs	91.82 ± 3.87	100	104.9 ± 14.63	388
NPC/V2a Aggs	96.16 ± 0.81	36.55 ± 1.63	124.35 ± 20.09	498

Values presented as mean ± standard deviation.
Aggs, aggregates.

impact force preset to 200 kD (actual force: 264 ± 68 kD). Upon injury, 96.9% of animals displayed a lateralized bruise, while the rest (3.1%) either had a more medial bruise or the view was obstructed due to a severe subdural bleed. With regard to disruption of the anterior vessel and associated subdural hemorrhage, animals exhibited severe (15.6%) moderate (15.6%), mild (23.3%) or no (45.5%) subdural bleeding. Most animals (71.9%) exhibited hindlimb and tail spasticity immediately after impact. All injured animals that experienced respiratory arrest ($n = 46$; 95.8% of total injured animals) were immediately intubated and mechanically ventilated for 1 h. A total of 6/48 (12.5%) of the animals either did not wean from the ventilator and died shortly after SCI (within 1 h of SCI) or did wean but did not recover post-injury due to respiratory complications (died within 1 week after SCI). The

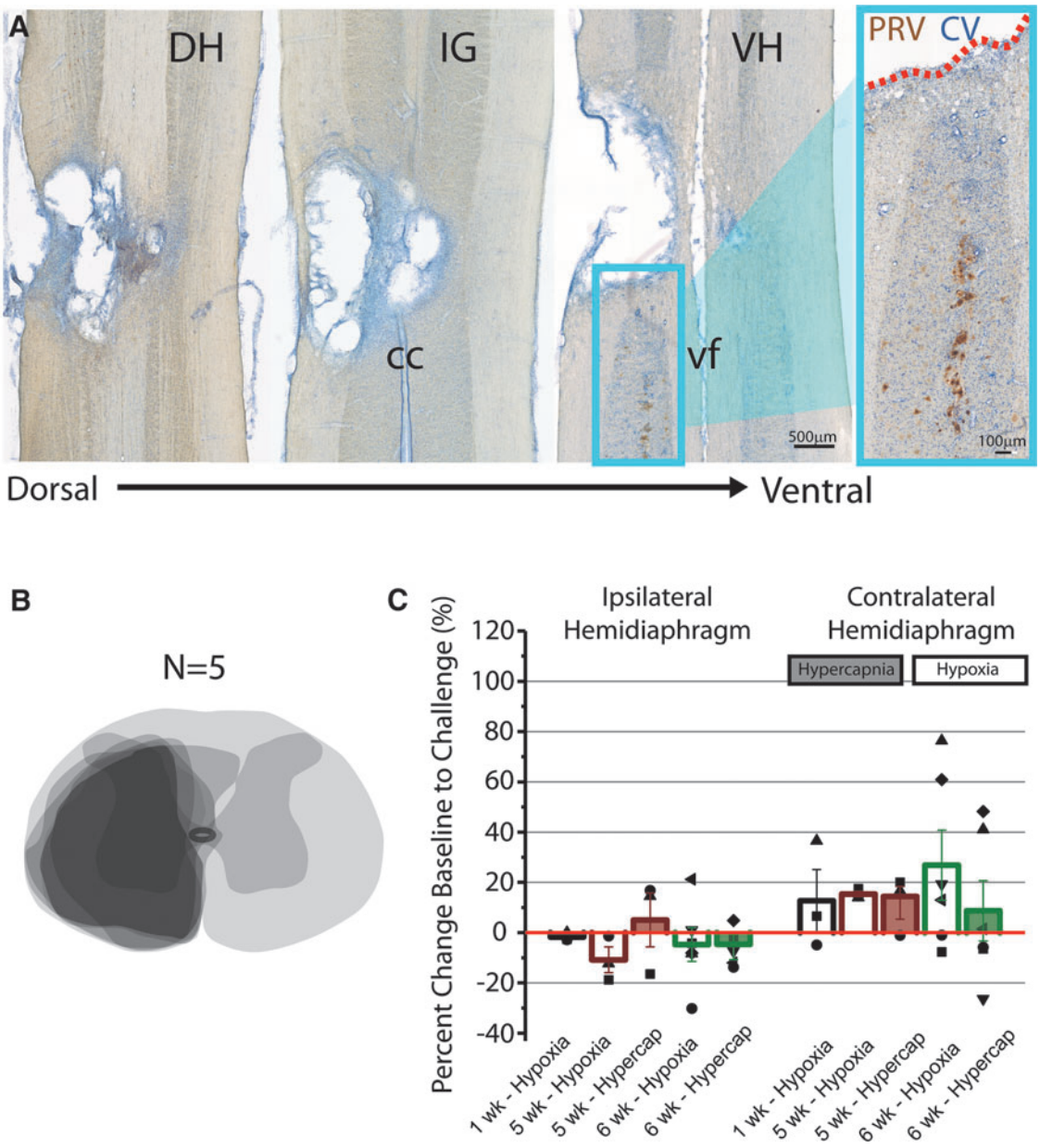

FIG. 4. Cervical level contusive injury results in anatomical and functional deficits. Horizontal sections stained with antibody against pseudorabies virus (PRV, brown) and counter stained with cresyl violet (CV, blue) through the injured (non-transplanted) cervical spinal cord 1 month after injury ranging from dorsal to ventral parts of the spinal cord **(A).** PRV labeling was used to retrogradely label the phrenic motor circuit, demonstrating that the injury is located primarily on the rostral-most part of the phrenic motor nucleus (A, inset). **(B)** An overlay of schematic diagrams of spinal cord cross sections of five injured animals through the lesion epicenter demonstrates reproducible anatomical damage 1 month after contusion injury. **(C)** Quantitative analysis of the change in diaphragm output as a response to hypoxic (non-shaded bar graphs) and hypercapnic (shaded bar graphs) respiratory challenges reveals the distribution of average diaphragm activity 1 ($n=3$), 5 ($n=3$), and 6 ($n=6$) weeks after injury. Each point represents the percent change of diaphragm output during a respiratory challenge for each individual animal that was able to survive 5 min of the challenge. Dotted line represents response to challenge seen in naïve (non-injured), age-matched animals. Scale bars are as indicated. DH, dorsal horn; IG, intermediate gray; VH, ventral horn; cc; central canal; vf; ventral fissure.

transplantation paradigm used in this study is sub-acute (1 week after injury shown in Fig. 1G), increasing the risk of morbidity and mortality in a population of injured, respiratory compromised, animals. An additional seven of remaining 42 animals (16.7%) did not recover after transplantation surgery and either died overnight or had to be sacrificed due to post-surgical complications (i.e., apparent respiratory problems such as gasping and inability to eat). Altogether, 35 transplant-recipients were available for analysis.

Horizontal sections stained against the transneuronal, retrograde tracer PRV, which labels phrenic moto- and interneurons, were used to anatomically confirm the location (rostral part of the phrenic motor nucleus) of the injury (Fig. 4A). Schematic diagrams of spinal cord cross sections of five injured animals through the lesion epicenter demonstrates reproducible anatomical damage 1 month after contusion injury (Fig. 4B). Diaphragm activity (electromyography) was recorded 1, 5, and 6 weeks after injury, revealing a consistent inability to increase diaphragm output when presented with a respiratory challenge, comparable to that reported previously.[12] Respiratory challenges were induced by exposure to hypoxic (Fig. 4C, unshaded bars) or hypercapnic (Fig. 4C, shaded bar graphs) gas. Each symbol represents the average amplitude of breaths recorded from either ipsilateral or contralateral hemidiaphragm over 40 sec from each animal, while each bar graph represents the average response to challenge of the group. Whereas naïve animals have been reported to increase diaphragm output approximately 75% compared with baseline,[12] injured animals displayed a consistent insufficiency of the hemidiaphragm on the side of injury (Fig. 4C), with no significant differences between each time-point or challenge used.

Survival, extension, and migration of transplanted cells

To track the survival and development of transplanted NPCs into the contusion cavity, anatomical assessment was performed 3 days ($n=2$), 1 week ($n=2$), and 2 weeks ($n=1$) post-transplantation of donor cells. Transplanted NPCs survive but remain immature (nestin positive) 3 days and 1 week post-transplant, with very little nestin labeling at the 2-week time-point (Fig. 5A-C). While no donor cells are positive for the mature astrocytic marker (GFAP) 3 days post-transplantation (Fig. 5D), there are numerous examples of expression seen by 1 and 2 weeks (Fig. 5E and 5F, respectively). While there is little evidence for NeuN (FOX3) labeling within 3 days post-transplantation (Fig. 5G), donor cells differentiate into NeuN positive neurons as early as 1 week (Fig. 5H), with examples of excitatory (vGLUT1) and inhibitory (GAD 67) neurons seen at 2 weeks (Fig. 5I, 5J).

Anatomical assessment 1 month post-transplantation revealed donor cell survival in all cell recipients, including NPC only (single-cell suspension or aggregated) and NPC/V2a IN transplants. The lesion and transplant volumes were found to be statistically similar between all groups ($p>0.05$; Fig. 6). Non-aggregated NPC transplants ($n=8$) were found to fill the injury cavity (43.7% ± 7.82%; Fig. 6A, 6E), extend axons both rostral (up to 6.3 mm) and caudal (up to 5.0 mm) as measured from the edge of transplant. Animals that received aggregated NPCs ($n=6$; Fig. 6B) and NPC/V2a IN aggregates ($n=8$; Fig. 6C) also filled the injury cavity and some of the lesioned tissue, although to a lesser extent when compared with non-aggregated NPC transplants (25.7% ± 6.15%; and 23.5% ± 4.20%, respectively; Fig. 6E). These transplants maintained aggregated structures within the animal after transplantation (Fig. 6B, 6C), presumably consistent with donor aggregates. Donor V2a's extended neurites both rostral (up to 8.6 mm) and caudal (up to 7.5 mm) as measured from the edge of the transplant.

In addition to the formation of aggregated structures within the lesion cavity, GFP-labeled cells were seen both rostral and caudal to the lesion boundary in all transplant recipients. The extent of this apparent ''migration'' was quantified. All detected migrating cells had a glial morphology (Fig. 7A), with prolonged cell body (29.8 μm ± 1.97 μm Feret diameter) and highly ramified processes. Immunostaining revealed negative reactivity to NeuN, GFAP, or RIP (markers for neurons, astrocytes or oligodendrocytes, respectively). These cells were found preferentially in ipsilateral white matter both rostral (Fig. 7A) and caudal (Fig. 7F-I′) to transplant epicenter, a migratory pattern reported previously for donor glial cells.[60,61] Interestingly, quantification of the percent of cells that migrated out from ''lesioned tissue'' was greater in the aggregated transplants compared with NPCs that were transplanted as single cells (50.8% ± 7.43% in NPC aggregates and 53.6% ± 4.76% in NPC/V2a IN transplants compared with 28.0% ± 4.35% in dissociated NPC transplants; Fig. 6E).

The cell bodies of TdTomato positive V2a INs were found only within the transplant aggregates as shown in Figure 7C-E, located ventral to the majority of observable TdTomato positive V2a IN projections (Fig. 7F-I), traversing host white matter. Such projections were found in white matter of the host both rostral (C2/rostral portion of C3 in Fig. 7B) and caudal (Fig. 7F-I′) to transplant epicenter. There was no evidence for V2a IN projections contralateral to the lesion/transplant.

Differentiation of transplanted cells

Consistent with previous findings, donor NPCs differentiated into NeuN positive neurons and GFAP positive astrocytes[45,60] in NPC-only transplants, as well as NPC/V2a IN transplants, as assessed at 1 month post-transplant (Fig. 8A-E). No V2a IN was observed to express GFAP. Some (12.2% ± 0.59%) of the transplanted V2a INs expressed NeuN (FOX3) marker (Fig. 8E, 8F; white arrowheads), and made up 11.4% ± 0.77% of total number of NeuN positive cells derived from donor cells, as quantified 1 month after transplantation (Fig. 8G). These V2a INs were larger in size, as measured by their Feret diameter maximum (20.7 μm ± 1.7μm) compared with V2a INs that were negative for NeuN staining (12.4 μm ± 0.68 μm). The majority of V2a INs that were positive for NeuN were in transplants found in the intermediate gray and ventral parts of the host cord, whereas V2a INs negative for NeuN were found throughout the transplant (Fig. 8E; red arrowheads). For comparison, NeuN positive neurons derived from NPCs (GFP positive) were measured to have an average Feret maximum of 23.1 μm ± 1.9 μm, and were found throughout the transplant (Fig. 8E; black arrowhead).

Proliferative capacity was assessed using an antibody against Ki67 with minimal (1–2% of Ki67 labeling detected in V2a INs *in vitro* prior to transplantation),[57] and no Ki67+/TdTomato+ cells detected in any transplant recipient 1 month post-transplant (Fig. 8H-K). Proliferating NPCs (Ki67+/GFP+), however, were found in all three transplant groups. Interestingly, most of these cells were located at the edge of transplanted aggregates, in close proximity to GFAP labeling (Fig. 8J, 8K; white arrowheads). As has been reported previously for similar NPC transplantation studies, there was no detectable tumorigenic-like growth in any animal.[60]

TdTomato (V2a IN projections) positive bouton-like formations were observed on GFP positive cells (putative donor neurons), as well as NeuN positive (GFP negative) cells (putative host cells). When stained against synaptophysin antibodies, synaptophysin positive, GFP negative (host) structures were found in close

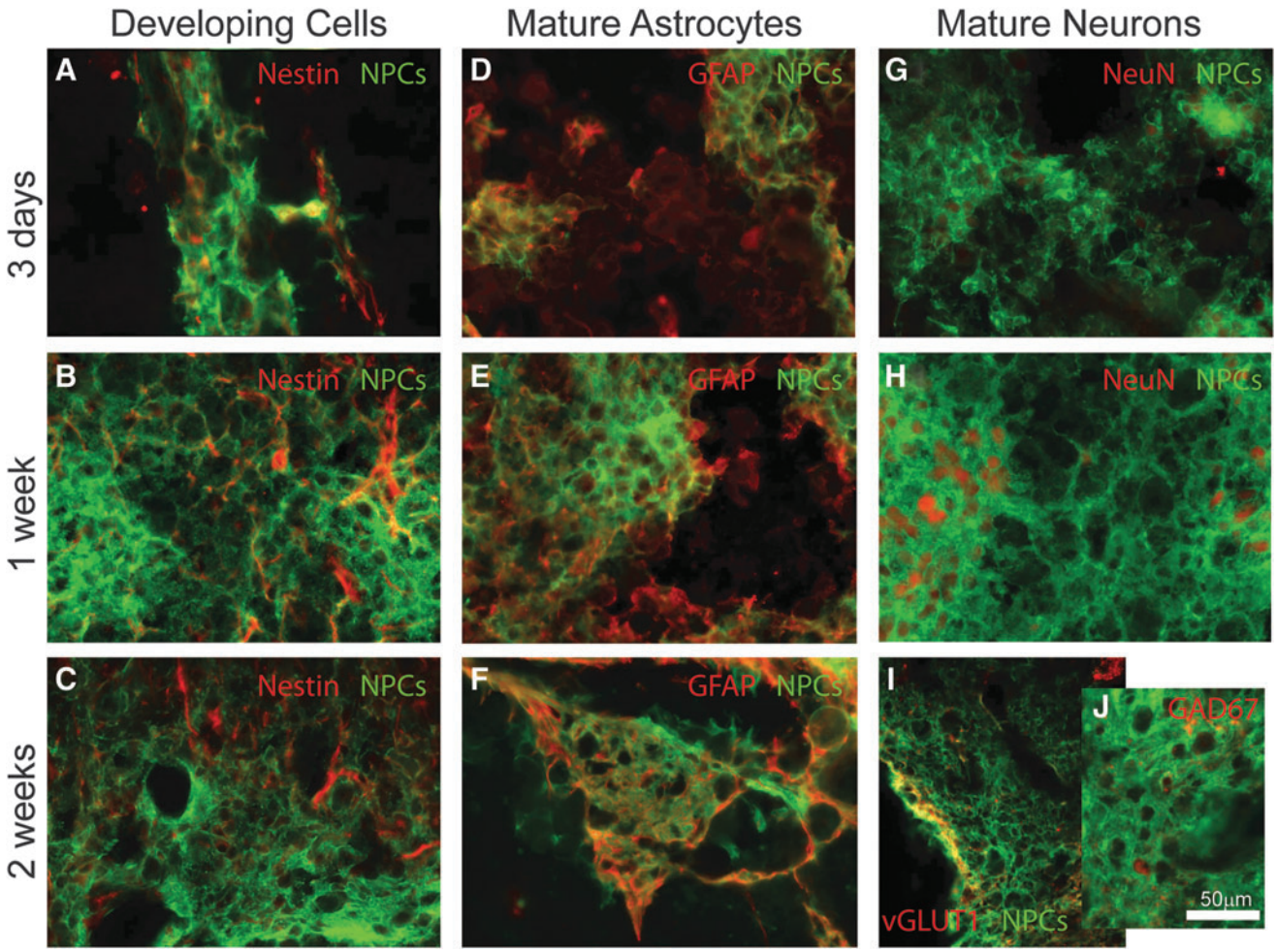

FIG. 5. Transplanted cultured neural progenitor cells (NPCs) survive and differentiate into neurons and glia. Transplanted cultured NPCs survive but remain immature (nestin positive) 3 days post-transplantation **(A).** Fewer donor cells are nestin positive by 1 week post-transplantation **(B),** and by 2 weeks, there is almost no expression of nestin within the transplant **(C).** While no donor cells are positive for the mature astrocytic marker (GFAP) 3 days post-transplantation **(D),** there are numerous examples of expression seen by 1 **(E)** and 2 weeks **(F).** While there is little evidence for NeuN (FOX3) labeling within 3 days post-transplantation **(G),** NeuN positive neurons are visible by 1 week **(H).** Tissue examined 2 weeks after transplantation reveals expression of excitatory (vGLUT1, **I**) and inhibitory (GAD67; **J**) markers. Scale bar is 50 microns.

proximity to V2a INs (putative host synapses onto V2a donor cells). Figure 8L shows examples of GFP negative synaptic formations around a NeuN positive V2a IN, suggesting synaptic formations from host neurons onto donor V2a INs.

Functional contribution of transplanted aggregates to diaphragm activity

Bilateral diaphragm activity was measured by dEMG 1 month after transplantation to assess functional contribution of transplanted cells in NPC (Fig. 9A; green traces) and NPC/V2a IN recipients (Fig. 9A; orange traces), compared with vehicle controls (Fig. 9A; black traces). Diaphragm activity was present in all animals (i.e., transplanted cells did not prevent spontaneous activity seen in control/vehicle animals) during eupnea or respiratory challenge. Single-cell and aggregated NPC transplant-recipients were statistically similar in all conditions; therefore, the data for the two groups were pooled together. Diaphragm amplitude of all transplant recipients, and their vehicle-control counterparts was recorded during eupneic (baseline) conditions, as well as during a 5-min period of a respiratory challenge induced by subjecting the animals to hypercapnic and hypoxic gases. The purpose of the 5-min respiratory challenges is to test the ability of the animals respond to the challenge by increasing diaphragm muscle output and subsequent ventilation. This method of increasing the respiratory drive has been used to reveal functional deficits that are not evident during a period of quiet, eupneic breathing.[59] Diaphragm activity recorded during baseline (eupnea) on the side of the injury was significantly greater in NPC/V2a recipients (0.19 ± 0.02 mV), compared with either NPC (0.14 ± 0.01 mV) or vehicle (0.077 ± 0.02 mV) controls ($p < 0.05$ for all comparisons; Fig. 9B).

Diaphragm amplitude recorded during respiratory challenges (hypoxia and hypercapnia) revealed similar patterns of activity on the side of the injury, with greatest amplitude in NPC/V2a IN recipients (0.22 ± 0.02 mV hypoxia; 0.22 ± 0.03 mV hypercapnia), compared with either NPC (0.14 ± 0.01 mV hypoxia; 0.14 ± 0.01 mV hypercapnia) or vehicle (0.07 ± 0.03 mV hypoxia; 0.08 ± 0.03 mV hypercapnia) controls (Fig. 9C, 9D). All numerical dEMG data for both

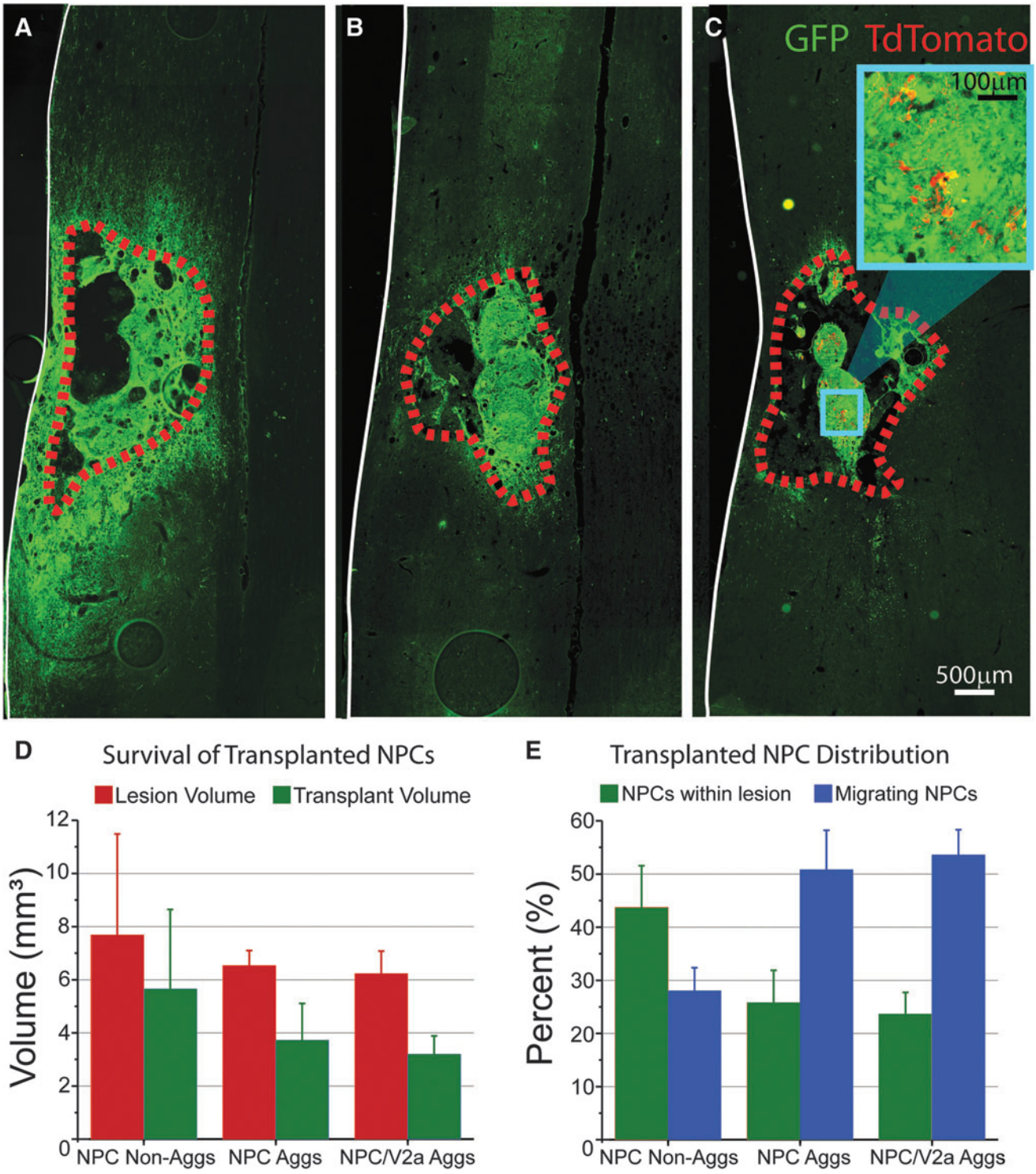

FIG. 6. Transplanted neural progenitor cells (NPCs) and NPC/V2a interneuron aggregates (Aggs) survive 1 month post-transplantation. Horizontal sections through epicenters of single-cell suspended (non-aggregated, **A**) and aggregated **(B)** NPCs, and NPC/V2a interneuron (IN) Aggs **(C).** Quantitative analysis of lesion volume and transplanted NPCs **(D)** reveals similar lesion and transplant volumes across all groups, but different distributions (within lesioned tissue versus migrated) of transplanted NPCs **(E).** Scale bars are as indicated. $*p \leq 0.05$, analysis of variance.

hemidiaphragms as well physiological data (oxygen saturation and heart rate) are summarized in Table 4. Quantitative analysis of the change in diaphragm output as a response to hypoxic or hypercapnic respiratory challenge are summarized in Figure 9E, 9F, showing no significant differences in this outcome measure.

Discussion

Since the late 19th century, transplantation of fetal tissue has been performed with the objective of creating neuronal relays capable of bypassing the injury site to regenerate endogenous

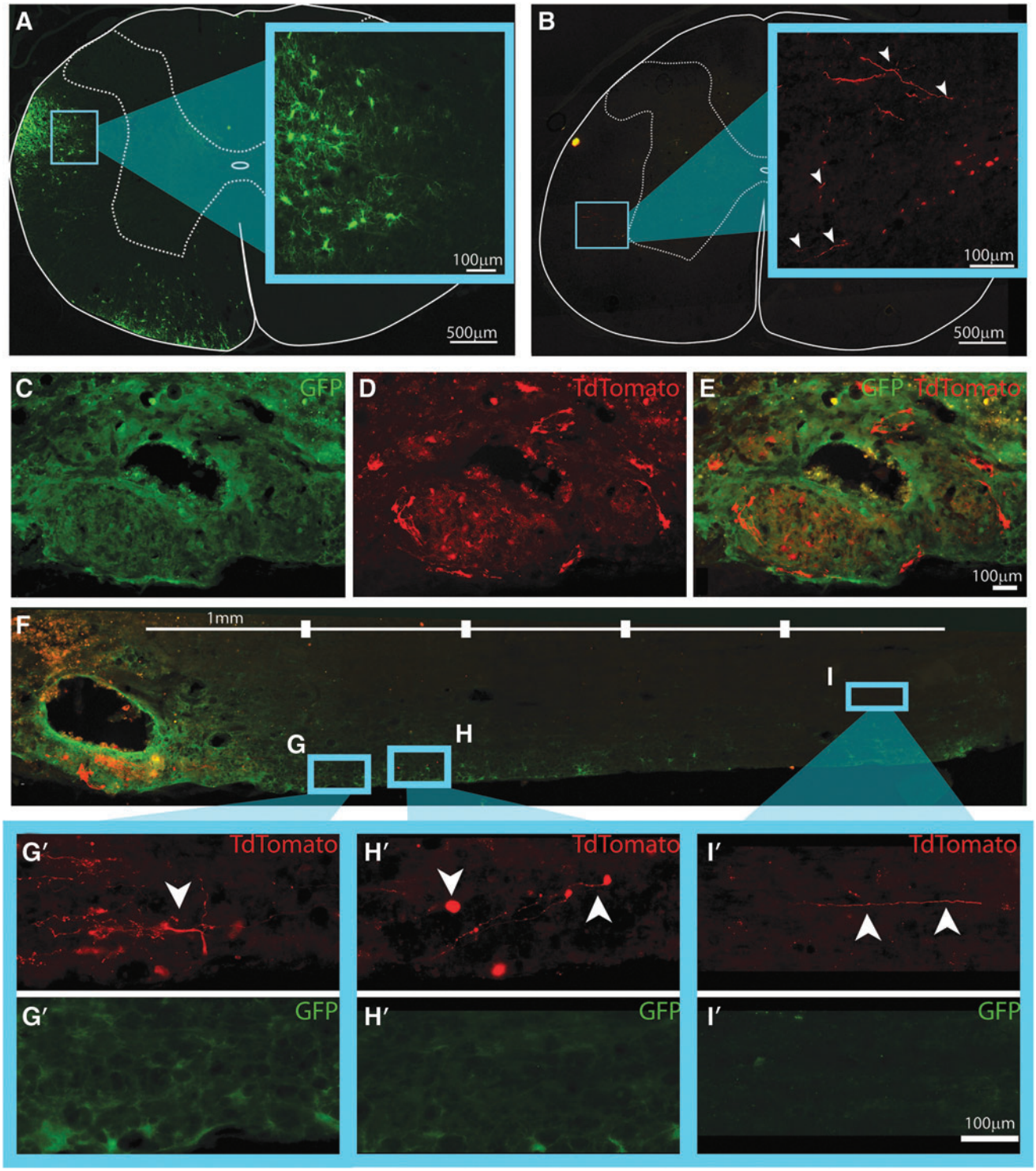

FIG. 7. Transplanted neural progenitor cells (NPCs) and NPC/V2a interneuron aggregates (Aggs) migrate and extend neurite projections 1 month after transplantation. Cross-sections of NPC/V2a (interneuron) IN transplant-recipients show examples of migrating NPCs **(A)** and V2a IN neurite outgrowth rostral to injury and transplant epicenter **(B)**. Cell bodies of V2a INs were found in transplanted Agg epicenters within the intermediate gray of the injured host spinal cord **(C-E)** with neurite extensions traversing host white matter **(F).** High powered images of V2a IN projections (white arrowheads) and migrating NPCs **(G-I′)**. Scale bars are as indicated.

circuits.[36,47,62] The lessons learned from fetal grafts, such as the optimal source and age of embryonic tissue, the capacity for cell survival, outgrowth, connectivity, and functional contribution to host circuitry, have been invaluable to the rapidly growing field of cell transplantation for repair of the injured central nervous system. Pre-clinical data have also led to clinical translation with reports of safety, feasibility, and potential for beneficial outcomes,[63,64] and spurred a growing interest in isolating, culturing, creating a bankable cell source, and characterizing these refined NPCs both *in vitro*[49,60,65] and after transplantation.[45,60,66]

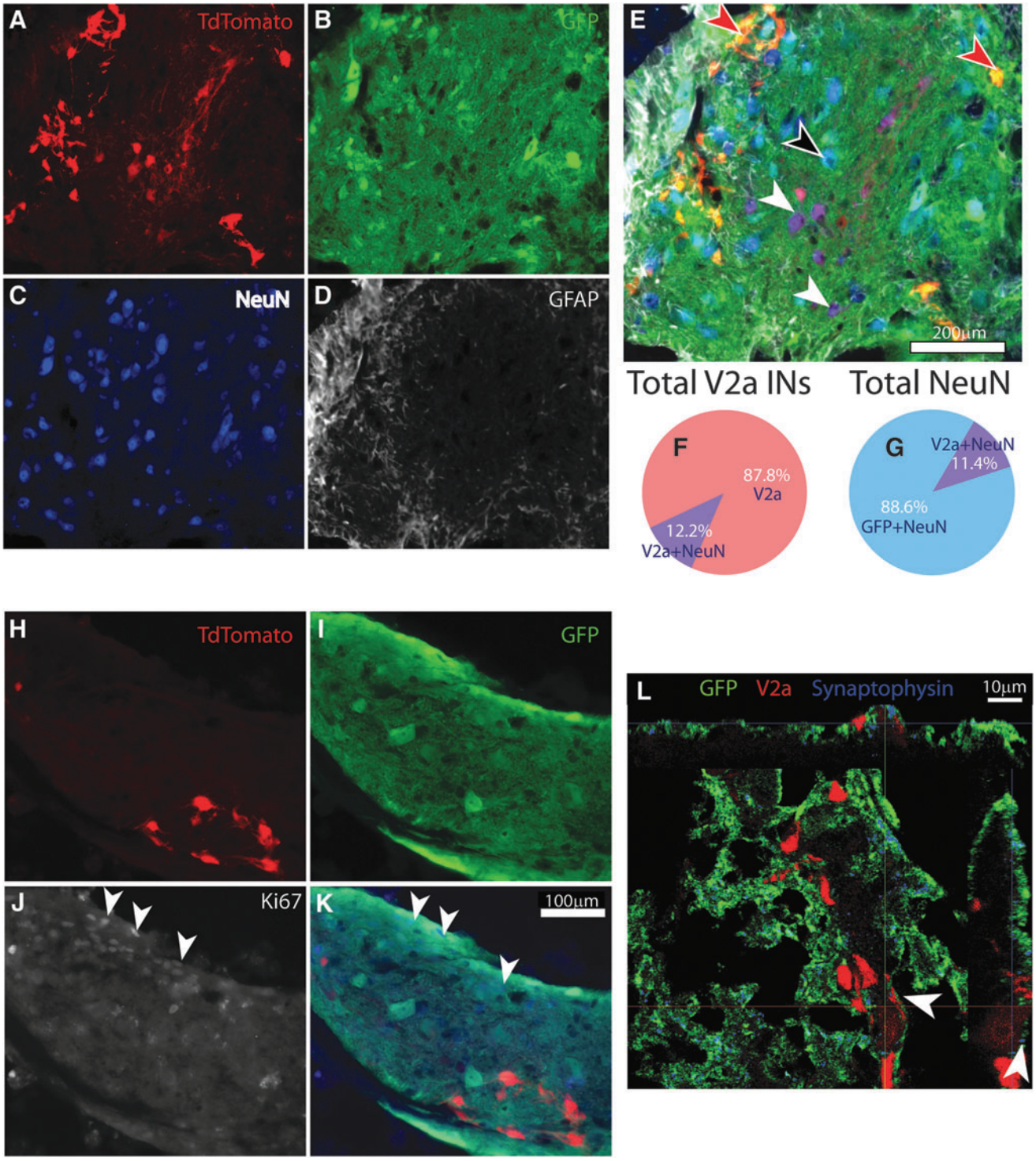

FIG. 8. Transplanted neural progenitor cells (NPCs)/V2a interneuron (IN) aggregates differentiate into mature neurons and glia. Horizontal section through the lesion/transplant epicenter of a NPC/V2a IN aggregate-transplant showing TdTomato positive V2a INs **(A),** GFP positive NPCs **(B)**, stained with NeuN **(C)** to visualize mature neurons, and glial fibrillary acidic protein (GFAP; **D**) to visualize astrocytes. Overlay of (A-D) is depicted in **(E)**. Black arrowhead points to a mature (NeuN positive) neuron from NPCs, while white arrowheads point to mature (NeuN positive) V2a INs. Red arrowheads point to NeuN negative, TdTomato positive V2a INs. Quantification of the number of V2a INs that were also positive for NeuN as percent of total number of V2a INs counted **(F)** and as the total number of NeuN positive neurons within GFP positive transplant **(G)**. **(H-K)** shows a similar section of NPC/V2a IN aggregate, stained for Ki67 (white in J; blue in K), showing proliferative capacity of NPCs, but not V2a INs (white arrowheads in J and K). **(L)** Confocal orthogonal image of a host (GFP and TdTomato negative) synapse (synaptophysin, blue), onto V2a IN (TdTomato, red). Scale bars are as indicated.

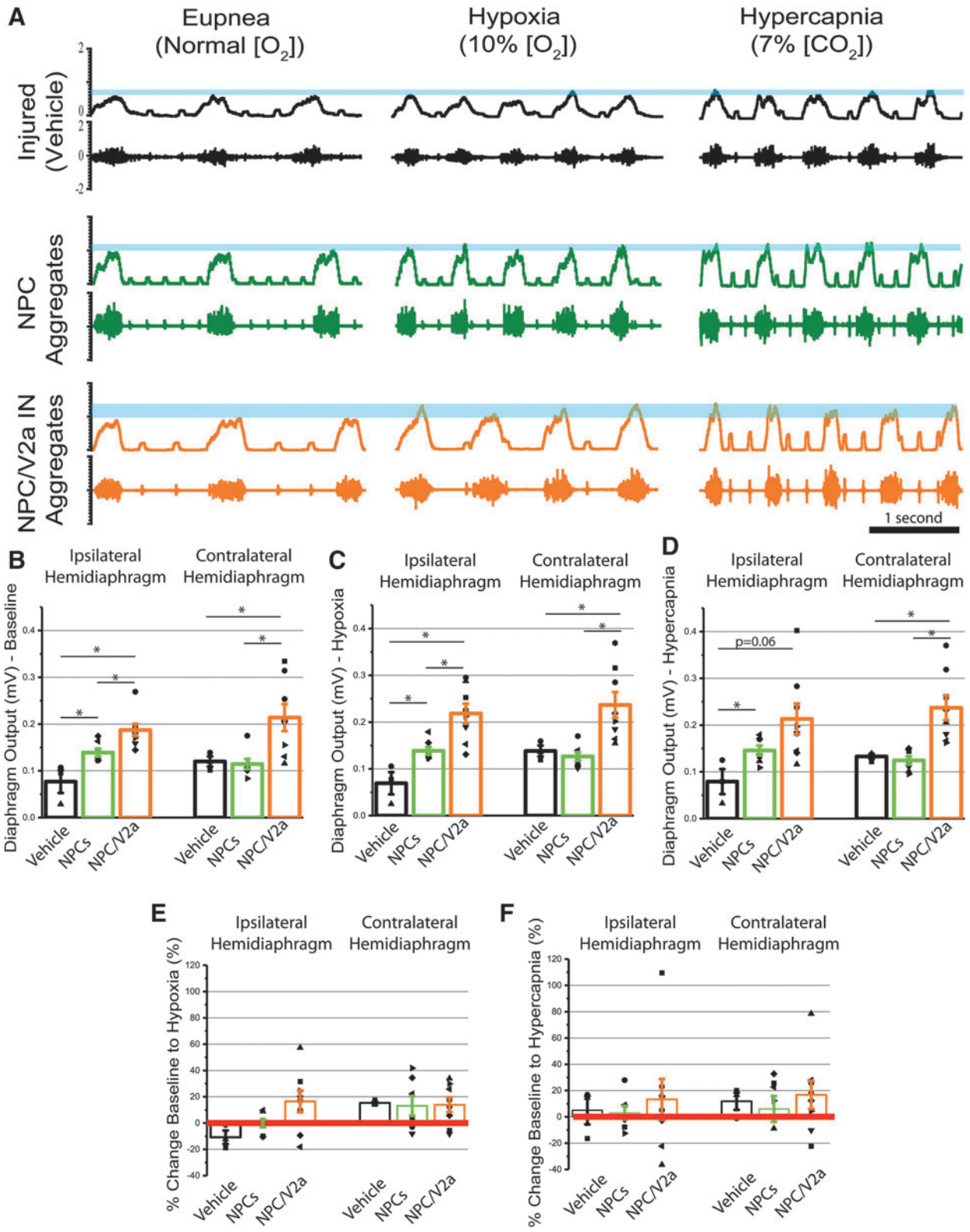

FIG. 9. Electromyogram recordings of diaphragm activity reveals modulation of activity in transplant recipients. Representative traces of muscle recordings of ipsilateral to injury and vehicle/transplant hemidiaphragm electromyography (EMG) 1 month post-injury in vehicle-treated controls (**A,** black), recipients of neural progenitor cells (NPC) Aggregates (Aggs) (A, green) and NPC/V2a interneurons (INs) INs (A, orange), during eupneic and challenged (hypoxia, hypercapnia) breathing. Blue lines in (A) represent output change between baseline (eupnea) and respiratory challenge (hypoxia, hypercapnia) in each group. Quantitative analysis of average diaphragm output during baseline (eupneic, **B**), or challenged breathing (hypoxia in **C** and hypercapnia in **D**) reveals statistically significant differences in transplant recipients compared with vehicle-controls. Recipients of V2a-enriched NPCs showed greater recovery than those with NPCs alone. Percent change baseline to hypoxia **(E)** and hypercapnia **(F)** reveals the distribution of average diaphragm activity for each animal and variability among each group. Each dot represents an individual animal's average diaphragm output over a 40-sec time span at the end of the respiratory challenge. Vehicle ($n=3$), NPCs ($n=7$), NPC/V2a INs ($n=8$); $*p \leq 0.05$, Student's *t*-test.

Table 4. Quantification of Vitals and Ipsilateral and Contralateral Hemidiaphragm Activity during Eupnea, Hypoxia, and Hypercapnia

Group	*Condition*	*Ipsilateral hemidiaphragm output (mV)*	*Contralateral hemidiaphragm output (mV)*	*SpO_2 (%)*	*Heart rate (BPM)*	*Breathing frequency (breaths per min)*
Vehicle	Eupnea	0.0769 ± 0.0245	0.1200 ± 0.0109	94.9 ± 0.1	175.8 ± 5.9	49.5 ± 4.0
NPCs	Eupnea	0.1391 ± 0.0082	0.1145 ± 0.0108	94.3 ± 0.8	182.4 ± 5.2	39.0 ± 2.8
NPCs/V2a	Eupnea	0.1896 ± 0.0149	0.2223 ± 0.0318	93.7 ± 0.8	179.1 ± 7.4	42.9 ± 2.7
Vehicle	Hypoxia	0.0693 ± 0.0236	0.1382 ± 0.0116	80.4 ± 3.7	172.4 ± 19.8	87.0 ± 3.1
NPCs	Hypoxia	0.1385 ± 0.0081	0.1266 ± 0.0089	79.3 ± 2.0	186.5 ± 7.5	75.2 ± 6.1
NPCs/V2a	Hypoxia	0.2193 ± 0.0243	0.2418 ± 0.0313	79.9 ± 1.4	172.6 ± 9.4	76.5 ± 5.2
Vehicle	Hypercapnia	0.0791 ± 0.0268	0.1329 ± 0.0056	96.7 ± 0.5	167.0 ± 9.3	63.0 ± 3.8
NPCs	Hypercapnia	0.1434 ± 0.0136	0.1210 ± 0.0116	96.7 ± 0.4	166.0 ± 4.5	52.9 ± 3.2
NPCs/V2a	Hypercapnia	0.2154 ± 0.0383	0.2478 ± 0.0281	96.0 ± 0.5	169.4 ± 6.1	55.9 ± 2.7
Percent change to hypoxia						
		Ipsilateral hemidiaphragm	Contralateral hemidiaphragm			
Vehicle		−10.8 ± 5.1	15.4 ± 1.1			
NPCs		−0.1 ± 3.0	13.0 ± 7.4			
NPCs/V2a		15.3 ± 9.5	11.6 ± 5.9			
Percent change to hypercapnia (%)						
		Ipsilateral hemidiaphragm	Contralateral hemidiaphragm			
Vehicle		5.0 ± 10.7	11.9 ± 6.5			
NPCs		0.3 ± 3.9	11.9 ± 7.4			
NPCs/V2a		13.0 ± 17.9	18.5 ± 12.2			

BPM, breaths per minute; NPCs, neural progenitor cells.

The pre-clinical fetal graft experiments also have demonstrated that transplanted cells can retain their phenotype throughout development within the injured spinal cord, and may replace some interneuronal populations that are lost after an injury.[67,68] The identification of specific neural precursor cell subtypes that optimize repair and promote functional recovery of target circuits is a necessary next step. Although progress has been made to test transplantation of specific glial progenitor subtypes (e.g., oligodendrocyte progenitor cells), little effort has been made to identify neuronal progenitors optimal for circuit repair. This is likely due in part to the technical challenges of identifying interneuronal subtypes beyond excitatory, inhibitory or neuromodulatory phenotypes with molecular markers.[41,69,70] Building upon our recent identification of ventrallyderived excitatory V2a spinal interneurons (SpINs) as contributors to anatomical plasticity within the injured phrenic circuitry after high cervical spinal cord injury (SCI),[13] and the role of V2a INs in respiration,[19] as well as respiratory plasticity,[22] the present work for the first time 1) tests the therapeutic potential of cultured NPCs in a contusion model of SCI and 2) explores the feasibility of enriching these NPCs with V2a INs for transplantation into the injured spinal cord.

NPCs as a platform for circuit repair

The NPCs used in this study were isolated and expanded from E13-14 rat spinal cord,[48] and although the spinal cord at this developmental stage primarily (80–90%) consists of neuronal and glial restricted progenitors (NRPs and GRPs, respectively), it also contains a small population of neural stem cells, mature neurons (e.g. motoneurons that have extended projections to periphery), fibroblasts, endothelial cells, and associated extracellular matrix.[49,60,71,72] The isolation and culturing process used here (adherent culture on poly-L-lysine and laminin coated substrate) reproducibly refines the donor populations to neuronal and glial progenitors[49] that have a capacity for self-renewal but restricted differentiation fate (e.g., only become neurons or glial cells).[60,65] Although these NPCs have been demonstrated to be successful in reconnecting the interrupted sensory system,[45] transplanted cells survived poorly in a more severe injury (complete thoracic transection) despite a combination of variety of matrices (Vitrogen, Matrigel, fibrin) and even 3- to 9-day delay in transplantation,[73] and have not been tested in a moderate-severe cervical contusion model.

Here, we test the therapeutic potential of cultured NPCs in a relevant injury model (contusion) and of a clinically important system (respiration). Similar to previous studies, NPCs survived within the cystic cavity of a contusion and progressively downregulated the expression of immature markers such as nestin, increasing markers of mature excitatory and inhibitory neurons and glia (Fig. 5).[45,60] Transplanted NPCs also contributed to functional circuit recovery as measured by diaphragm electromyography during baseline breathing (Fig. 9B) and during respiratory challenges (Fig. 9C, 9D). This offers further evidence that NPCs can be used as a platform for spinal cord repair, providing the building block necessary for creating spinal networks.

V2a INs and respiration

The ventrally derived Chx10-driven V2a INs play a vast number of roles in the spinal cord. These excitatory, ipsilaterally projecting INs have been extensively studied within the lumbar spinal cord (in the context of the central pattern generator) and role in locomotion. For example, V2a INs contribute to the descending inputs that organize left-right alternation during normal[18] and high-speed locomotion.[20,74–76] These INs are heterogeneous on the transcriptional[77] and functional levels[21,78] having both local and long-range projections and the ability to synapse onto motoneurons or commissural INs.[18,79,80] Despite having a consistent distribution throughout the rostro-caudal axis of the spinal cord,[77] much less in known about the

role of V2a INs in the cervical spinal cord. Among the studies that have investigated the cells within the cervical cord, these cells have been shown to help control skilled reaching[15] and play a role in respiratory plasticity.[13,22]

Within the respiratory circuit, genetic ablation of the V2a INs located in the medial reticular formation results in early neonatal death and irregular breathing in surviving mice.[19] These V2a INs project to neurons in the pre-Bötzinger complex, a center for respiratory drive.[81] Apart from their direct influence over the pre-Bötzinger complex, V2a INs located in the cervical spinal cord play a role in compensatory respiratory plasticity, as these cells have been implicated to have a crucial role for the recruitment of accessory respiratory muscles in a mouse model of amyotrophic lateral sclerosis.[22] Further, the V2a INs located in the spinal cord contribute to anatomic phrenic plasticity, as we have recently shown the recruitment of V2a INs into injured phrenic pathways following high cervical SCI.[13]

Identifying V2a interneurons as a potential candidate for transplantation

In experiments transplanting whole, dorsally or ventrally derived embryonic spinal cord tissue into the injured cervical spinal cord and denervated phrenic motor circuit, White and colleagues[38] found that ventrally derived spinal tissue (basal plate) exhibited some therapeutic efficacy, whereas spontaneous plasticity and functional recovery was attenuated in recipients of dorsally derived tissue. This raises concern over the potential for transplanting cells that are not only ineffectual but detrimental to recovery of motor circuits. Thus, it is necessary to begin assessing which cells are capable of repairing specific injured circuits and contributing to recovery and equally important, which donor progenitors might prevent recovery or exacerbate deficits.

Advances in cell culture techniques have allowed for the identification of cells present in fetal tissue (i.e., neural precursor and progenitor cells in the E13.5-14 rat spinal cord),[49,50,82] and subsequently allowed for the isolation, storage and use of such cell populations in pre-clinical models of SCI.[48,60,83,84] However, how these isolation techniques influence the phenotypic development of NPCs has not been well characterized. The present study demonstrates that the isolation and culturing process necessary to obtain a refined and bankable source of NPCs for transplantation attenuates the ventrally derived Chx10-driven (V2a) class of INs. Given these observations, the present work tested the hypothesis that enriching the NPC population with V2a INs and transplanting the combination of the cells would provide a more effective cell population (much like what has been found, albeit indirectly, by White and colleagues)[38] and further enhance respiratory recovery after SCI.

Recent studies by Brown and colleagues[85] and Butts and colleagues[86] showed that post-mitotic V2a INs can be generated from either mouse embryonic stem cells (ESCs) or human pluripotent stem cells. Both studies employed a combination of small molecules in specific temporal sequences that have been shown to play a role in patterning the neural tube during development to drive the expression of ventral transcriptional factors. These differentiation protocols yielded heterogeneous population of cells, including of neuronal and glial lineages, with enriched numbers of Chx10-expressing V2a INs. Subsequent studies by Iyer and colleagues[57] generated a selectable mouse ESC line by using defined transcription factor promoters (in the case of V2a INs the transcriptional factor is Chx10) that drive puromycin resistance. This allowed for the selection of V2a INs specifically by driving ventral signaling pathways and then subjecting differentiated cells to puromycin, thus identifying a method for producing very highly enriched (e.g., 80% Chx10+ and 94% Lhx3+) populations of post-mitotic V2a INs that can be used for controlled *in vitro* (e.g., functions of different IN populations within ''circuitoids,'' much like was done in the study by Sternfeld and colleagues)[87] and *in vivo* studies (e.g., transplantation of defined populations of INs into the injured spinal cord to repair neural circuits). Iyer and colleagues[57] demonstrated that these selected V2a INs mature into excitatory glutamatergic (Vglut2+) neurons (MAP2+) after 2 weeks in culture, and display electrophysiological properties that are consistent with work on native V2a cells.[21,88] When co-cultured with glial cells and putative motoneurons, V2a INs derived form Chx10-Puro ESCs have been shown to make functional excitatory synapses (e.g., blocked evoked transmission with administration of AMPA/kainite receptor antagonist, NBQX) onto each other and onto putative motoneurons, similar to characteristics of V2a's that has been demonstrated *in vivo* in the context of locomotion[18,20,21,88] and respiration.[19,22]

ESC-V2a INs are viable candidates for cell transplantation

In this study, we used Chx10-Puro mouse ESC-derived V2a INs[57] to enrich NPCs derived from the rat embryonic spinal cord[45,48,60] and assess efficacy following transplantation into a moderate-severe contusion SCI. We hypothesized that seeding the post-mitotic mouse V2a INs with NPCs at a 1:1 ratio will provide the necessary supporting environment for these cells to survive the inhibitory environment characteristic of the injury epicenter. Based on this 1:1 aggregation, while donor V2a's comprised half of all donor cells (neuronal and glial), they represent majority of donor neuronal precursors (roughly 3:1 ratio). Here, we demonstrate the feasibility of transplanting these cellular aggregates into the lesion cavity that forms 1 week after a cervical contusion injury. Donor post-mitotic V2a INs survive after transplantation, do not stain for the proliferation marker Ki67, and do not generate tumor-like growths.[60,89] To the best of our knowledge, robust survival of post-mitotic neurons in the injured spinal cord has not been previously reported, in fact some studies presented evidence to the contrary,[34] even when transplanted with supporting glia. The ideal age of cells for transplantation to survive in the inhibitory milieu of an injury have been identified between embryonic Day 12–15 in the rat[34] (e.g., when most of the spinal cells are at the progenitor stage of development, not post-mitotic),[90] serving as the justification for follow up studies by us[41] and others.[35–39,42,62,67,68,70,91,92]

Despite attaining robust survival of post-mitotic V2a INs when combined with NPCs, only some (12.2%) of the transplanted V2a INs expressed mature neuronal markers such as NeuN (FOX3), suggesting that future studies should incorporate a longer end-point to assess maturity and connectivity of these cells. These results are different from the results reported in Butts and colleagues with transplantation of unselected human pluripotent cell-derived V2a INs into the uninjured spinal cord, where 91% of Chx10+ INs also expressed NeuN.[86] The main and most important difference, however, between the present data and results demonstrated in Butts and colleagues[86] is that the present data consist of transplanting into the injured spinal cord, which has been demonstrated to inhibit donor cell maturation.[93] Of all donor cells that become mature NeuN-positive neurons 1 month post-transplantation, 11.4% are from donor V2a INs. While it is possible that donor V2a cells also become FOX3-negative mature neurons, the fact that not all donor V2a INs might have matured is an important consideration for correlating

functional outcomes to the anatomical results in the present work. For instance, while functional improvement was seen in some recipients of V2a-enriched NPCs, not all animals displayed the same level of recovery. Thus, an important consideration is that these donor cells may need longer than 1 month to mature and form stable connections with the injured host circuitry. This is why future studies will assess whether donor cells continue to proliferate and integrate with host neurons at even later times (3, 6, or 12 months). Nevertheless, the presence of GFP negative (i.e., host, not donor), synaptophysin positive vesicles on transplanted V2a IN cell bodies suggests that the host spinal cord innervates transplanted V2a INs.

Despite the preservation of interpenetrating networks of neurites after transplantation (Fig. 8A), TdTomato positive neurites (putative axons) were seen extending several millimeters into the host spinal cord, as has been reported recently following transplantation into the uninjured spinal cord.[86] This confirms the potential for transplanted V2a INs to extend projections into host spinal cord and synapse onto host interneurons and motoneurons. This also opens the possibility for directing V2a IN outgrowth towards a specific target by using either viral methods (as in 94)[94] or with activity based therapies that are known to elicit the production of neurotrophic factors within the spinal cord.[95]

Conclusion

The present work has revealed that culturing cells isolated from the developing spinal cord alters expression of interneuronal transcription factors, and accordingly may alter the population of spinal interneurons available in donor tissues. While there is a significant decrease in transcription factors associated with V2a spinal interneurons—cells known to contribute to plasticity after cervical SCI[13]—enriching donor cells with stem cell–derived V2a neurons improves functional outcome. Overall, this study demonstrates the feasibility of transplanting a selected population of neurons in combination with neural progenitor cells (NPCs) into a moderate cervical spinal cord injury model for respiratory dysfunction. Survival, extension, migration, and differentiation were observed, although maturation in these populations remained minimal 1 month post-transplantation. However, functional recovery was significantly greater in a subset of animals that received V2a-enriched NPCs, over NPCs alone.

Future studies will employ longer end-points that allow for enhanced maturation and integration of these transplanted cells, enhancing potential contribution to functional recovery. Future studies should also employ chemogenetic strategies to selectively silence transplanted V2a INs and specifically investigate their functional contribution to phrenic recovery. Transynaptic tracing can be used to define the extent of connectivity and how connectivity correlates to functional outcomes. Future studies could also employ the use of scaffolds to enhance survival and differentiation of post-mitotic neurons post-transplantation.[96] As the number of pre-clinical and clinical studies using NPCs to repair the central nervous system continues to grow, there is a clear need for more thorough characterization of donor cell phenotypes, assessment of donor cell survival and differentiation after transplantation, and determination of transplant contribution to functional improvement. With the knowledge that some donor neurons may adversely affect functional outcome, yet others—like the V2a's used here—333333333may beneficially enhance recovery, greater effort will need to be made to establish which cells will best serve to promote recovery post-SCI, and tailor transplants to treat specific motor and sensory systems.

Acknowledgments

This work was funded by the National Institute of Neurological Disorders and Stroke, NIH R01 NS081112 (Lane), NIH R01 NS090617 (Sakiyama-Elbert), NIH, P01 NS 055976 Project 2 (Fischer), NIH NRSA F31 NS090760 (Iyer), Craig H. Neilsen (#338432, Lane; #381793, Qiang), the Lisa Dean Moseley Foundation (Lane), the Drexel Deans Fellowship for Collaborative or Themed Research (Zholudeva) and the Spinal Cord Research Center at Drexel University, College of Medicine. PRV614 was produced and supplied by Dr. David Bloom (University of Florida). Primary antibodies to PRV were supplied by Dr. Lynn Enquist (Princeton University) as part of Virus Center funding (P40 RR018604) awarded to Dr. Enquist. The content is solely the responsibility of the authors and does not necessarily represent the official views of the National Institutes of Health.

Author Disclosure Statement

No competing financial interests exist.

References

1. Fuller, D.D., Doperalski, N.J., Dougherty, B.J., Sandhu, M.S., Bolser, D.C., and Reier, P.J. (2008). Modest spontaneous recovery of ventilation following chronic high cervical hemisection in rats. Exp. Neurol. 211, 97–106.
2. Fuller, D.D., Golder, F.J., Olson, E.B., and Mitchell, G.S. (2006). Recovery of phrenic activity and ventilation after cervical spinal hemisection in rats. J. Appl. Physiol. (1985) 100, 800–806.
3. Vinit, S., Stamegna, J.C., Boulenguez, P., Gauthier, P., and Kastner, A. (2007). Restorative respiratory pathways after partial cervical spinal cord injury: role of ipsilateral phrenic afferents. Eur. J. Neurosci. 25, 3551–3560.
4. Fuller, D.D., Johnson, S.M., Olson, E.B., and Mitchell, G.S. (2003). Synaptic pathways to phrenic motoneurons are enhanced by chronic intermittent hypoxia after cervical spinal cord injury. J. Neurosci. 23, 2993–3000.
5. Golder, F.J. and Mitchell, G.S. (2005). Spinal synaptic enhancement with acute intermittent hypoxia improves respiratory function after chronic cervical spinal cord injury. J. Neurosci. 25, 2925–2932.
6. Nantwi, K.D., El-Bohy, A.A., Schrimsher, G.W., Reier, P.J., and Goshgarian, H. (1999). Spontaneous functional recovery in a paralyzed hemidiaphragm following upper cervical spinal cord injury in adult rats. Neurorehabil. Neural Repair 13, 225–234.
7. Golder, F.J., Reier, P.J., Davenport, P.W., and Bolser, D.C. (2001). Cervical spinal cord injury alters the pattern of breathing in anesthetized rats. J. Appl. Physiol. (1985) 91, 2451–2458.
8. Bareyre, F.M., Kerschensteiner, M., Raineteau, O., Mettenleiter, T.C., Weinmann, O., and Schwab, M.E. (2004). The injured spinal cord spontaneously forms a new intraspinal circuit in adult rats. Nat. Neurosci. 7, 269–277.
9. Courtine, G., Song, B., Roy, R.R., Zhong, H., Herrmann, J.E., Ao, Y., Qi, J., Edgerton, V.R., and Sofroniew, M.V. (2008). Recovery of supraspinal control of stepping via indirect propriospinal relay connections after spinal cord injury. Nat. Med. 14, 69–74.
10. Courtine, G., Gerasimenko, Y., van den Brand, R., Yew, A., Musienko, P., Zhong, H., Song, B., Ao, Y., Ichiyama, R.M., Lavrov, I., Roy, R.R., Sofroniew, M.V., and Edgerton, V.R. (2009). Transformation of nonfunctional spinal circuits into functional states after the loss of brain input. Nat. Neurosci. 12, 1333–1342.
11. Fouad, K. and Tse, A. (2008). Adaptive changes in the injured spinal cord and their role in promoting functional recovery. Neurol. Res. 30, 17–27.
12. Lane, M.A., Lee, K.Z., Salazar, K., O'Steen, B.E., Bloom, D.C., Fuller, D.D., and Reier, P.J. (2012). Respiratory function following bilateral mid-cervical contusion injury in the adult rat. Exp. Neurol. 235, 197–210.
13. Zholudeva, L.V., Karliner, J.S., Dougherty, K.J., and Lane, M.A. (2017). Anatomical recruitment of spinal V2a interneurons into phrenic motor circuitry after high cervical spinal cord injury. J. Neurotrauma 34, 3058–3065.

14. Sandhu, M.S., Dougherty, B.J., Lane, M.A., Bolser, D.C., Kirkwood, P.A., Reier, P.J., and Fuller, D.D. (2009). Respiratory recovery following high cervical hemisection. Respir. Physiol. Neurobiol. 169, 94–101.
15. Azim, E., Jiang, J., Alstermark, B., and Jessell, T.M. (2014). Skilled reaching relies on a V2a propriospinal internal copy circuit. Nature 508, 357–363.
16. Bouvier, J., Caggiano, V., Leiras, R., Caldeira, V., Bellardita, C., Balueva, K., Fuchs, A., and Kiehn, O. (2015). Descending command neurons in the brainstem that halt locomotion. Cell 163, 1191–1203.
17. Bretzner, F. and Brownstone, R.M. (2013). Lhx3-Chx10 reticulospinal neurons in locomotor circuits. J. Neurosci. 33, 14681–14692.
18. Crone, S.A., Quinlan, K.A., Zagoraiou, L., Droho, S., Restrepo, C.E., Lundfald, L., Endo, T., Setlak, J., Jessell, T.M., Kiehn, O., and Sharma, K. (2008). Genetic ablation of V2a ipsilateral interneurons disrupts left-right locomotor coordination in mammalian spinal cord. Neuron 60, 70–83.
19. Crone, S.A., Viemari, J.C., Droho, S., Mrejeru, A., Ramirez, J.M., and Sharma, K. (2012). Irregular breathing in mice following genetic ablation of V2a neurons. J. Neurosci. 32, 7895–7906.
20. Crone, S.A., Zhong, G., Harris-Warrick, R., and Sharma, K. (2009). In mice lacking V2a interneurons, gait depends on speed of locomotion. J. Neurosci. 29, 7098–7109.
21. Zhong, G., Droho, S., Crone, S.A., Dietz, S., Kwan, A.C., Webb, W.W., Sharma, K., and Harris-Warrick, R.M. (2010). Electrophysiological characterization of V2a interneurons and their locomotor-related activity in the neonatal mouse spinal cord. J. Neurosci. 30, 170–182.
22. Romer, S.H., Seedle, K., Turner, S.M., Li, J., Baccei, M.L., and Crone, S.A. (2016). Accessory respiratory muscles enhance ventilation in ALS model mice and are activated by excitatory V2a neurons. Exp. Neurol. 287(Pt 2), 192–204
23. Mantilla, C.B., Bailey, J.P., Zhan, W.Z., and Sieck, G.C. (2012). Phrenic motoneuron expression of serotonergic and glutamatergic receptors following upper cervical spinal cord injury. Exp. Neurol. 234, 191–199.
24. Alilain, W.J. and Goshgarian, H.G. (2008). Glutamate receptor plasticity and activity-regulated cytoskeletal associated protein regulation in the phrenic motor nucleus may mediate spontaneous recovery of the hemidiaphragm following chronic cervical spinal cord injury. Exp. Neurol. 212, 348–357.
25. Alilain, W.J. and Goshgarian, H.G. (2007). MK-801 upregulates NR2A protein levels and induces functional recovery of the ipsilateral hemidiaphragm following acute C2 hemisection in adult rats. J. Spinal Cord Med. 30, 346–354.
26. Streeter, K.A., Sunshine, M.D., Patel, S., Gonzalez-Rothi, E.J., Reier, P.J., Baekey, D.M., and Fuller, D.D. (2017). Intermittent hypoxia enhances functional connectivity of midcervical spinal interneurons. J. Neurosci. 37, 8349–8362.
27. Cregg, J.M., Chu, K.A., Hager, L.E., Maggard, R.S.J. and Stoltz, D.R.E., M.Alilain, W.J.Philippidou, P.Landmesser, L.T.Silver, J. (2017). A latent propriospinal network can restore diaphragm function after high cervical spinal cord injury. Cell Rep. 21, 654–665.
28. Fuller, D.D., Sandhu, M.S., Doperalski, N.J., Lane, M.A., White, T.E., Bishop, M.D., and Reier, P.J. (2009). Graded unilateral cervical spinal cord injury and respiratory motor recovery. Respir. Physiol. Neurobiol. 165, 245–253.
29. Choi, H., Liao, W.L., Newton, K.M., Onario, R.C., King, A.M., Desilets, F.C., Woodard, E.J., Eichler, M.E., Frontera, W.R., Sabharwal, S., and Teng, Y.D. (2005). Respiratory abnormalities resulting from midcervical spinal cord injury and their reversal by serotonin 1A agonists in conscious rats. J. Neurosci. 25, 4550–4559.
30. Golder, F.J., Fuller, D.D., Lovett-Barr, M.R., Vinit, S., Resnick, D.K., and Mitchell, G.S. (2011). Breathing patterns after mid-cervical spinal contusion in rats. Exp. Neurol. 231, 97–103.
31. Conta Steencken, A.C. and Stelzner, D.J. (2010). Loss of propriospinal neurons after spinal contusion injury as assessed by retrograde labeling. Neuroscience 170, 971–980.
32. Conta Steencken, A.C., Smirnov, I., and Stelzner, D.J. (2011). Cell survival or cell death: differential vulnerability of long descending and thoracic propriospinal neurons to low thoracic axotomy in the adult rat. Neuroscience 194, 359–371.
33. Siebert, J.R., Middleton, F.A., and Stelzner, D.J. (2010). Long descending cervical propriospinal neurons differ from thoracic propriospinal neurons in response to low thoracic spinal injury. BMC Neurosci. 11, 148.
34. Reier, P.J., Perlow, M.J., and Guth, L. (1983). Development of embryonic spinal cord transplants in the rat. Brain Res. 312, 201–219.
35. Reier, P.J. (1985). Neural tissue grafts and repair of the injured spinal cord. Neuropathol. Appl. Neurobiol. 11, 81–104.
36. Reier, P.J., Bregman, B.S., and Wujek, J.R. (1986). Intraspinal transplantation of embryonic spinal cord tissue in neonatal and adult rats. J. Comp. Neurol. 247, 275–296.
37. Jakeman, L.B. and Reier, P.J. (1991). Axonal projections between fetal spinal cord transplants and the adult rat spinal cord: a neuroanatomical tracing study of local interactions. J. Comp. Neurol. 307, 311–334.
38. White, T.E., Lane, M.A., Sandhu, M.S., O'Steen, B.E., Fuller, D.D., and Reier, P.J. (2010). Neuronal progenitor transplantation and respiratory outcomes following upper cervical spinal cord injury in adult rats. Exp. Neurol. 225, 231–236.
39. Lee, K.Z., Lane, M.A., Dougherty, B.J., Mercier, L.M., Sandhu, M.S., Sanchez, J.C., Reier, P.J., and Fuller, D.D. (2014). Intraspinal transplantation and modulation of donor neuron electrophysiological activity. Exp. Neurol. 251, 47–57.
40. Lin, C.C., Lai, S.R., Shao, Y.H., Chen, C.L., and Lee, K.Z. (2017). The therapeutic effectiveness of delayed fetal spinal cord tissue transplantation on respiratory function following mid-cervical spinal cord injury. Neurotherapeutics 14, 792–809.
41. Spruance, V.M., Zholudeva, L.V., Hormigo, K.M., Randelman, M.L., Bezdudnaya, T., Marchenko, V., and Lane, M.A. (2018). Integration of transplanted neural precursors with the injured spinal cord. J. Neurotrauma 35, 1781–1799.
42. Lu, P., Wang, Y., Graham, L., McHale, K., Gao, M., Wu, D., Brock, J., Blesch, A., Rosenzweig, E.S., Havton, L.A., Zheng, B., Conner, J.M., Marsala, M., and Tuszynski, M.H. (2012). Long-distance growth and connectivity of neural stem cells after severe spinal cord injury. Cell 150, 1264–1273.
43. Lu, P., Graham, L., Wang, Y., Wu, D., and Tuszynski, M. (2014). Promotion of survival and differentiation of neural stem cells with fibrin and growth factor cocktails after severe spinal cord injury. J. Vis. Exp. e50641.
44. Lu, P., Kadoya, K., and Tuszynski, M.H. (2014). Axonal growth and connectivity from neural stem cell grafts in models of spinal cord injury. Curr. Opin. Neurobiol. 27, 103–109.
45. Bonner, J.F., Connors, T.M., Silverman, W.F., Kowalski, D.P., Lemay, M.A., and Fischer, I. (2011). Grafted neural progenitors integrate and restore synaptic connectivity across the injured spinal cord. J. Neurosci. 31, 4675–4686.
46. Reier, P.J. (2004). Cellular transplantation strategies for spinal cord injury and translational neurobiology. NeuroRx 1, 424–451.
47. Jakeman, L.B. and Reier, P.J. (2015). Fetal spinal cord transplantation after spinal cord injury: around and back again, in: *Neural Regeneration.* So, K.F. (ed). Elsevier Inc.: Amsterdam, the Netherlands.
48. Bonner, J.F., Haas, C.J., and Fischer, I. (2013). Preparation of neural stem cells and progenitors: neuronal production and grafting applications. Methods Mol. Biol. 1078, 65–88.
49. Cai, J., Wu, Y., Mirua, T., Pierce, J.L., Lucero, M.T., Albertine, K.H., Spangrude, G.J., and Rao, M.S. (2002). Properties of a fetal multipotent neural stem cell (NEP cell). Dev. Biol. 251, 221–240.
50. Mayer-Proschel, M., Kalyani, A.J., Mujtaba, T., and Rao, M.S. (1997). Isolation of lineage-restricted neuronal precursors from multipotent neuroepithelial stem cells. Neuron 19, 773–785.
51. Lane, M.A., Lee, K.Z., Fuller, D.D., and Reier, P.J. (2009). Spinal circuitry and respiratory recovery following spinal cord injury. Respir. Physiol. Neurobiol. 169, 123–132.
52. Darlot, F., Cayetanot, F., Gauthier, P., Matarazzo, V., and Kastner, A. (2012). Extensive respiratory plasticity after cervical spinal cord injury in rats: axonal sprouting and rerouting of ventrolateral bulbospinal pathways. Exp. Neurol. 236, 88–102.
53. Harkema, S.J. (2008). Plasticity of interneuronal networks of the functionally isolated human spinal cord. Brain Res. Rev. 57, 255–264.
54. Ford, T.W., Anissimova, N.P., Meehan, C.F., and Kirkwood, P.A. (2016). Functional plasticity in the respiratory drive to thoracic motoneurons in the segment above a chronic lateral spinal cord lesion. J. Neurophysiol. 115, 554–567.

55. Hansen, C.N., Faw, T.D., White, S., Buford, J.A., Grau, J.W., and Basso, D.M. (2016). Sparing of descending axons rescues interneuron plasticity in the lumbar cord to allow adaptive learning after thoracic spinal cord injury. Front. Neural Circuits 10, 11.
56. Flynn, J.R., Graham, B.A., Galea, M.P., and Callister, R.J. (2011). The role of propriospinal interneurons in recovery from spinal cord injury. Neuropharmacology 60, 809–822.
57. Iyer, N.R., Huettner, J.E., Butts, J.C., Brown, C.R., and Sakiyama-Elbert, S.E. (2016). Generation of highly enriched V2a interneurons from mouse embryonic stem cells. Exp. Neurol. 277, 305–316.
58. Lane, M.A., White, T.E., Coutts, M.A., Jones, A.L., Sandhu, M.S., Bloom, D.C., Bolser, D.C., Yates, B.J., Fuller, D.D., and Reier, P.J. (2008). Cervical prephrenic interneurons in the normal and lesioned spinal cord of the adult rat. J. Comp. Neurol. 511, 692–709.
59. Fuller, D.D., Mitchell, G.S. and, Bavis, R.W. (2005). *Respiratory Neuroplasticity: Respiratory Gases, Development, and Spinal Injury.* Taylor and Francis: Boca Raton, FL.
60. Lepore, A.C. and Fischer, I. (2005). Lineage-restricted neural precursors survive, migrate, and differentiate following transplantation into the injured adult spinal cord. Exp. Neurol. 194, 230–242.
61. Han, S.S., Liu, Y., Tyler-Polsz, C., Rao, M.S., and Fischer, I. (2004). Transplantation of glial-restricted precursor cells into the adult spinal cord: survival, glial-specific differentiation, and preferential migration in white matter. Glia 45, 1–16.
62. Bregman, B.S. and Reier, P.J. (1986). Neural tissue transplants rescue axotomized rubrospinal cells from retrograde death. J. Comp. Neurol. 244, 86–95.
63. Thompson, F.J., Reier, P.J., Uthman, B., Mott, S., Fessler, R.G., Behrman, A., Trimble, M., Anderson, D.K., and Wirth, E.D. (2001). Neurophysiological assessment of the feasibility and safety of neural tissue transplantation in patients with syringomyelia. J. Neurotrauma 18, 931–945.
64. Wirth, E.D., Reier, P.J., Fessler, R.G., Thompson, F.J., Uthman, B., Behrman, A., Beard, J., Vierck, C.J., and Anderson, D.K. (2001). Feasibility and safety of neural tissue transplantation in patients with syringomyelia. Journal of neurotrauma 18, 911–929.
65. Han, S.S., Kang, D.Y., Mujtaba, T., Rao, M.S., and Fischer, I. (2002). Grafted lineage-restricted precursors differentiate exclusively into neurons in the adult spinal cord. Exp. Neurol. 177, 360–375.
66. Lepore, A.C., Neuhuber, B., Connors, T.M., Han, S.S., Liu, Y., Daniels, M.P., Rao, M.S., and Fischer, I. (2006). Long-term fate of neural precursor cells following transplantation into developing and adult CNS. Neuroscience 139, 513–530.
67. Jakeman, L.B., Reier, P.J., Bregman, B.S., Wade, E.B., Dailey, M., Kastner, R.J., Himes, B.T., and Tessler, A. (1989). Differentiation of substantia gelatinosa-like regions in intraspinal and intracerebral transplants of embryonic spinal cord tissue in the rat. Exp. Neurol. 103, 17–33.
68. Dulin, J.N., Adler, A.F., Kumamaru, H., Poplawski, G.H.D., Lee-Kubli, C., Strobl, H., Gibbs, D., Kadoya, K., Fawcett, J.W., Lu, P., and Tuszynski, M.H. (2018). Injured adult motor and sensory axons regenerate into appropriate organotypic domains of neural progenitor grafts. Nat. Commun. 9, 84.
69. Lin, C.C., Lai, S.R., Shao, Y.H., Chen, C.L., and Lee, K.Z. (2017). The therapeutic effectiveness of delayed fetal spinal cord tissue transplantation on respiratory function following mid-cervical spinal cord injury. Neurotherapeutics 14, 792–809.
70. Adler, A.F., Lee-Kubli, C., Kumamaru, H., Kadoya, K., and Tuszynski, M.H. (2017). Comprehensive monosynaptic rabies virus mapping of host connectivity with neural progenitor grafts after spinal cord injury. Stem Cell Rep. 8, 1525–1533.
71. Kalyani, A., Hobson, K. and Rao, M.S. (1997). Neuroepithelial stem cells from the embryonic spinal cord: isolation, characterization, and clonal analysis. Dev Biol 186, 202–223.
72. Mujtaba, T., Piper, D.R., Kalyani, A., Groves, A.K., Lucero, M.T., and Rao, M.S. (1999). Lineage-restricted neural precursors can be isolated from both the mouse neural tube and cultured ES cells. Dev. Biol. 214, 113–127.
73. Medalha, C.C., Jin, Y., Yamagami, T., Haas, C., and Fischer, I. (2014). Transplanting neural progenitors into a complete transection model of spinal cord injury. J Neurosci Res 92, 607–618.
74. Al-Mosawie, A., Wilson, J.M., and Brownstone, R.M. (2007). Heterogeneity of V2-derived interneurons in the adult mouse spinal cord. Eur. J. Neurosci. 26, 3003–3015.
75. Lundfald, L., Restrepo, C.E., Butt, S.J., Peng, C.Y., Droho, S., Endo, T., Zeilhofer, H.U., Sharma, K., and Kiehn, O. (2007). Phenotype of V2-derived interneurons and their relationship to the axon guidance molecule EphA4 in the developing mouse spinal cord. Eur. J. Neurosci. 26, 2989–3002.
76. Zhong, G., Sharma, K., and Harris-Warrick, R.M. (2011). Frequency-dependent recruitment of V2a interneurons during fictive locomotion in the mouse spinal cord. Nat Commun 2, 274.
77. Francius, C., Harris, A., Rucchin, V., Hendricks, T.J., Stam, F.J., Barber, M., Kurek, D., Grosveld, F.G., Pierani, A., Goulding, M., and Clotman, F. (2013). Identification of multiple subsets of ventral interneurons and differential distribution along the rostrocaudal axis of the developing spinal cord. PLoS One 8, e70325.
78. Dougherty, K. and Kiehn, O. (2010). Functional organization of V2a-related locomotor circuits in the rodent spinal cord. Ann. N. Y. Acad. Sci. 85–93.
79. Dougherty, K.J. and Kiehn, O. (2010). Functional organization of V2a-related locomotor circuits in the rodent spinal cord. Ann. N. Y. Acad. Sci. 1198, 85–93.
80. Zhong, G., Shevtsova, N.A., Rybak, I.A., and Harris-Warrick, R.M. (2012). Neuronal activity in the isolated mouse spinal cord during spontaneous deletions in fictive locomotion: insights into locomotor central pattern generator organization. J. Physiol. 590, 4735–4759.
81. Feldman, J.L., Mitchell, G.S., and Nattie, E.E. (2003). Breathing: rhythmicity, plasticity, chemosensitivity. Annu. Rev. Neurosci. 26, 239–266.
82. Rao, M.S., Noble, M., and Mayer-Proschel, M. (1998). A tripotential glial precursor cell is present in the developing spinal cord. Proc. Natl. Acad. Sci. U.S.A. 95, 3996–4001.
83. Lepore, A.C., Neuhuber, B., Connors, T.M., Han, S.S., Liu, Y., Daniels, M.P., Rao, M.S., and Fischer, I. (2006). Long-term fate of neural precursor cells following transplantation into developing and adult CNS. Neuroscience 142, 287–304.
84. Mitsui, T., Shumsky, J.S., Lepore, A.C., Murray, M., and Fischer, I. (2005). Transplantation of neuronal and glial restricted precursors into contused spinal cord improves bladder and motor functions, decreases thermal hypersensitivity, and modifies intraspinal circuitry. J. Neurosci. 25, 9624–9636.
85. Brown, C.R., Butts, J.C., McCreedy, D.A., and Sakiyama-Elbert, S.E. (2014). Generation of v2a interneurons from mouse embryonic stem cells. Stem Cells Dev. 23, 1765–1776.
86. Butts, J.C., McCreedy, D.A., Martinez-Vargas, J.A., Mendoza-Camacho, F.N., Hookway, T.A., Gifford, C.A., Taneja, P., Noble-Haeusslein, L., and McDevitt, T.C. (2017). Differentiation of V2a interneurons from human pluripotent stem cells. Proc. Natl. Acad. Sci. U.S.A. 114, 4969–4974.
87. Sternfeld, M.J., Hinckley, C.A., Moore, N.J., Pankratz, M.T., Hilde, K.L., Driscoll, S.P., Hayashi, M., Amin, N.D., Bonanomi, D., Gifford, W.D., Sharma, K., Goulding, M., and Pfaff, S.L. (2017). Speed and segmentation control mechanisms characterized in rhythmically-active circuits created from spinal neurons produced from genetically-tagged embryonic stem cells. Elife 6.
88. Dougherty, K.J. and Kiehn, O. (2010). Firing and cellular properties of V2a interneurons in the rodent spinal cord. J. Neurosci. 30, 24–37.
89. Johnson, P.J., Tatara, A., McCreedy, D.A., Shiu, A., and Sakiyama-Elbert, S.E. (2010). Tissue-engineered fibrin scaffolds containing neural progenitors enhance functional recovery in a subacute model of SCI. Soft Matter 6, 5127–5137.
90. Rao, M.S. (1999). Multipotent and restricted precursors in the central nervous system. Anat. Rec. 257, 137–148.
91. Reier, P.J., Houle, J.D., Jakeman, L., Winialski, D., and Tessler, A. (1988). Transplantation of fetal spinal cord tissue into acute and chronic hemisection and contusion lesions of the adult rat spinal cord. Progr. Brain Res. 78, 173–179.
92. Kadoya, K., Lu, P., Nguyen, K., Lee-Kubli, C., Kumamaru, H., Yao, L., Knackert, J., Poplawski, G., Dulin, J.N., Strobl, H., Takashima, Y., Biane, J., Conner, J., Zhang, S.C., and Tuszynski, M.H. (2016). Spinal

cord reconstitution with homologous neural grafts enables robust corticospinal regeneration. Nat. Med. 22, 479–487
93. Cao, Q.L., Howard, R.M., Dennison, J.B., and Whittemore, S.R. (2002). Differentiation of engrafted neuronal-restricted precursor cells is inhibited in the traumatically injured spinal cord. Exp. Neurol. 177, 349–359.
94. Bonner, J.F., Blesch, A., Neuhuber, B., and Fischer, I. (2010). Promoting directional axon growth from neural progenitors grafted into the injured spinal cord. J. Neurosci. Res. 88, 1182–1192.
95. Satriotomo, I., Dale, E.A., Dahlberg, J.M., and Mitchell, G.S. (2012). Repetitive acute intermittent hypoxia increases expression of proteins associated with plasticity in the phrenic motor nucleus. Exp. Neurol. 237, 103–115.
96. Thompson, R.E., Pardieck, J., Smith, L., Kenny, P., Crawford, L., Shoichet, M., and Sakiyama-Elbert, S. (2018). Effect of hyaluronic acid hydrogels containing astrocyte-derived extracellular matrix and/or V2a interneurons on histologic outcomes following spinal cord injury. Biomaterials 162, 208–223.

Address correspondence to:
Michael A. Lane, PhD
Department of Neurobiology and Anatomy
Drexel University
2900 W Queen Lane
Philadelphia, PA 19129

E-mail: mlane.neuro@gmail.com